

M V J COLLEGE OF ENGINEERING


Channasandra, Near Whitefield, Bangalore – 67




Department of Electronics and Communication


CERTIFICATE

Certified that the project work entitled “**Design And Development Of a 0.5-1.5 GHz Low Noise Cooled HEMT Amplifier**”, is a bonafide work carried out by *Deepankar-roy* and *Sharath.V.B* in partial fulfillment for the award of degree of Bachelor of Engineering in Electronics and Communication of the **Visveswatraiah Technological University**, Belgaum during the year 2003-04. It is certified that all corrections/suggestions indicated for internal Assessment have been incorporated in the Report deposited in the departmental library. The project report has been approved as it satisfies the academic requirements in respect of Project work prescribed for the Bachelor of Engineering Degree.


Signature of the Guide

Name of the student
Deepanakar-Roy
Sharath.V.B


Signature of the H.O.D
29-05-04
Head of Dept.
Electronics & Commn. Engg
M.V.J. College of Engineering
Bangalore - 560 067


Signature of the Principal
29/5
Principal
M.V.J. College of Engineering
Bangalore-560 067.
University Seat Number
1MJ00EC029
1MJ00EC094

External Viva

- 1.
- 2.

Name of the Examiners

Signature with date



May 25, 2004

Certificate

This is to certify that the project work entitled

***“Design & Development of a 0.5 to 1.5 GHz Low-noise Cooled HEMT
Amplifier”***

was carried out under my guidance by

Deepankar Roy

Sharath V.B.

students of the VIII semester, Bachelor of Engineering (Electronics & Communication), M.V.J. College of Engineering, Bangalore, in partial fulfillment of the requirement for the award of Bachelor's Degree in Electronics & Communication Engineering during the semester February 2004 – May 2004.

A. Raghunathan
Engineer

Radio Astronomy Laboratory

Abstract:

Astronomy is the field science involving the study of the nature of the Universe. The studies are carried out by investigating the radiation coming from the sky with the help of telescopes. In radio astronomy it is done for the radiation in the radio band of the electromagnetic spectrum with the help of radio telescopes.

The radio telescope collects the radiation emitted by the celestial object and amplifies it to detectable levels. The power levels of astronomical signals are in general extremely small and hence will be hidden completely in the man made noise.

A typical radio telescope consists of a feed, a low noise amplifier, heterodyne system and a detector. The signal collected by the feed is amplified and down converted before detecting it. The amplification is done in the low noise amplifier in such a manner that the signal to noise ratio of the incoming signal does not get worsened too much. Operating the amplifier at cryogenic temperature (77K) can minimize the thermal noise contribution of the amplifier.

Since every celestial body emits radiation at all frequencies, it is very much desirable to collect radiations at all those frequencies in order to characterize it over all those frequencies. This necessitates the amplifier to have as large operating bandwidth as possible with minimum noise contribution over it.

The main aim of the project is to build a low noise cryogenic amplifier having more than an octave bandwidth in the frequency range 0.5 to 1.5 GHz.

ACKNOWLEDGEMENT

First and foremost, we are thankful to Prof. N.Kumar, Director, Raman Research Institute for giving us an opportunity to work at RRI. Next, we are thankful to Mr. A.A. Sholapur, HOD, Dept. of Electronics and Communication, MVJCE, for giving us the permission to use this opportunity.

Next, we thank Dr.N.Udaya Shankar, HOD, *Radio Astronomy Lab* for his constant encouragement.

We express our sincere gratitude and profound thanks to our respectable guide Mr.A.Raghunathan, *Radio Astronomy Lab*, RRI, for his extensive and invaluable guidance.

We are thankful to Mrs. Sandhya, Ms. Kasturi, Mrs.Mamatha and Mrs.Arasi of *Radio Astronomy Lab* for their constant support. We sincerely thank Mr.K.B.Raghavendra and Mr.Sarabagopalan for their useful suggestions.

We thank Mr. Venugopal and Mr.Narayanaswamy of *basement workshop* for providing us the amplifier chassis.

We thank Mr. Raju Varghese for helping us with the photographs.

We also thank Dr. Patil- Librarian, RRI, for allowing us to use the library facilities.

We are also very thankful to our internal guide Mrs.Jyothi Deshmukh who showed utmost interest in our work and gave us extensive support.

CONTENTS

1. NOISE

1.1	Relevance of noise in radio astronomy	1
1.2	Basic definitions	7
1.3	General Receiver configuration in Radio Telescope	9
	1.3.1 Importance of Low Noise Amplifier in the Radio Receiver	10

2. DEVICE THEORY

2.1	Basic Definitions	11
2.2	Active devices	12
2.3	Description of various devices	13
	2.3.1 Microwave bipolar transistor	13
	2.3.2 Field effect transistor	15
	2.3.3 GaAs MESFET	17
	2.3.4 High electron mobility transistor (HEMT)	22

3. CIRCUIT THEORY

3.1	S-Parameters	25
	3.1.1 Introduction	25
	3.1.2 S-Parameters of a two port network	26
3.2	Power gain equations	28
3.3	Simultaneous conjugate matching	29
3.4	Stability circles and its importance	30
3.5	Constant gain circles	32
3.6	Noise model	34
	3.6.1 Application to noisy two port network	35
3.7	Dependence of noise factor on source admittance	37
3.8	Noise figure circles	39

4. CRYOGENICS

4.1 Effect of cooling on GaAs FET	41
4.2 Design aspects of the cooling system based on the cryocooler	46
4.3 Design of the housing for the low noise amplifier	47
4.4 Preliminary design of vacuum jacket	48
4.5 Estimation of thermal load to the cold head of the cryocooler	48
4.5.1 Heat transfer due to conduction	48
4.5.2 Heat transfer due to radiation	51

5. AMPLIFIER DESIGN

5.1 General amplifier block diagram	55
5.2 Selection of transistor	56
5.3 Stabilizing the transistor using feedback	57
5.3.1 stability factor	57
5.3.2 Lossless feedback	61
5.4 Design of matching sections	63
5.4.1 Design of input matching section	65
5.4.2 Design of interstage matching section	66
5.4.3 Design of output matching section	67
5.4.4 Modified design values after optimization	68
5.5 Design of bias section	71

6. BUILDING AND CHARACTERIZATION OF THE LOW NOISE AMPLIFIER

6.1 Construction details of the amplifier	72
6.1.1 Development of printed circuit board	72
6.1.2 Amplifier chassis	72
6.1.3 Amplifier assembling	74

6.2 Experimental setup for the measurement of Gain and Return Loss of the amplifier	77
6.3 Experimental setup for the measurement of Noise Figure of the amplifier	79

7. CONCLUSION

8. BIBLIOGRAPHY

9. APPENDIX

1.NOISE

1.1 Relevance of noise in radio astronomy

A Radio Telescope is a fundamental instrument used for the observation in Radio Astronomy. It basically consists of an antenna, a low noise receiver and a data recording system. The function of an antenna is to collect the radiation coming from the sky and convert it into a measurable signal. The receiver collects all the signals given by the antenna for processing. The processed signal is fed to the data recording system where the data gets stored for off line analysis.

When an antenna is pointed towards the sky, it receives not only the signal of our interest but also all the radiations mostly noise, falling within its operating frequency range. Since the strength of the signal emitted by an astronomical source will be extremely weak, it will be completely hidden within the noise received. Finally the capability of the receiver (Sensitivity) to detect the weakest signal depends upon the level of the noise received. It is highly desirable to keep the noise level as low as possible to achieve a highly sensitive radio receiver. It can be done either minimizing the noise level or by cryogenically cooling the front end of the receiver system.

There are three principal sources of noise – i) Environmental noise ii) Thermal noise and iii) receiver noise. Figure 1 shows the broad category of the sources of noise. Environmental noise mainly includes noise created by man, noise produced by the atmosphere and noise coming from the sky. Electrical disturbances from high tension wires and ignition in engines contribute mostly to the man made noise. Atmospheric noise contribution depends upon the frequency of observation. If it is a good absorber of radiation, it will be also a good emitter. There are also lots of sources in the sky emitting radiation. For example sun, radio stars and various diffuse radiations of galactic origin act as a wideband noise. As mentioned earlier, the receiver itself produces a large variety of noises like Johnson noise, shot noise, $1/f$ noise etc. In addition there are also other types of noises like quantization noise and quantum noise. These types of noises occur while digitizing the analog data output of the front end receiver of a radio telescope. A brief description of some of these is given below.

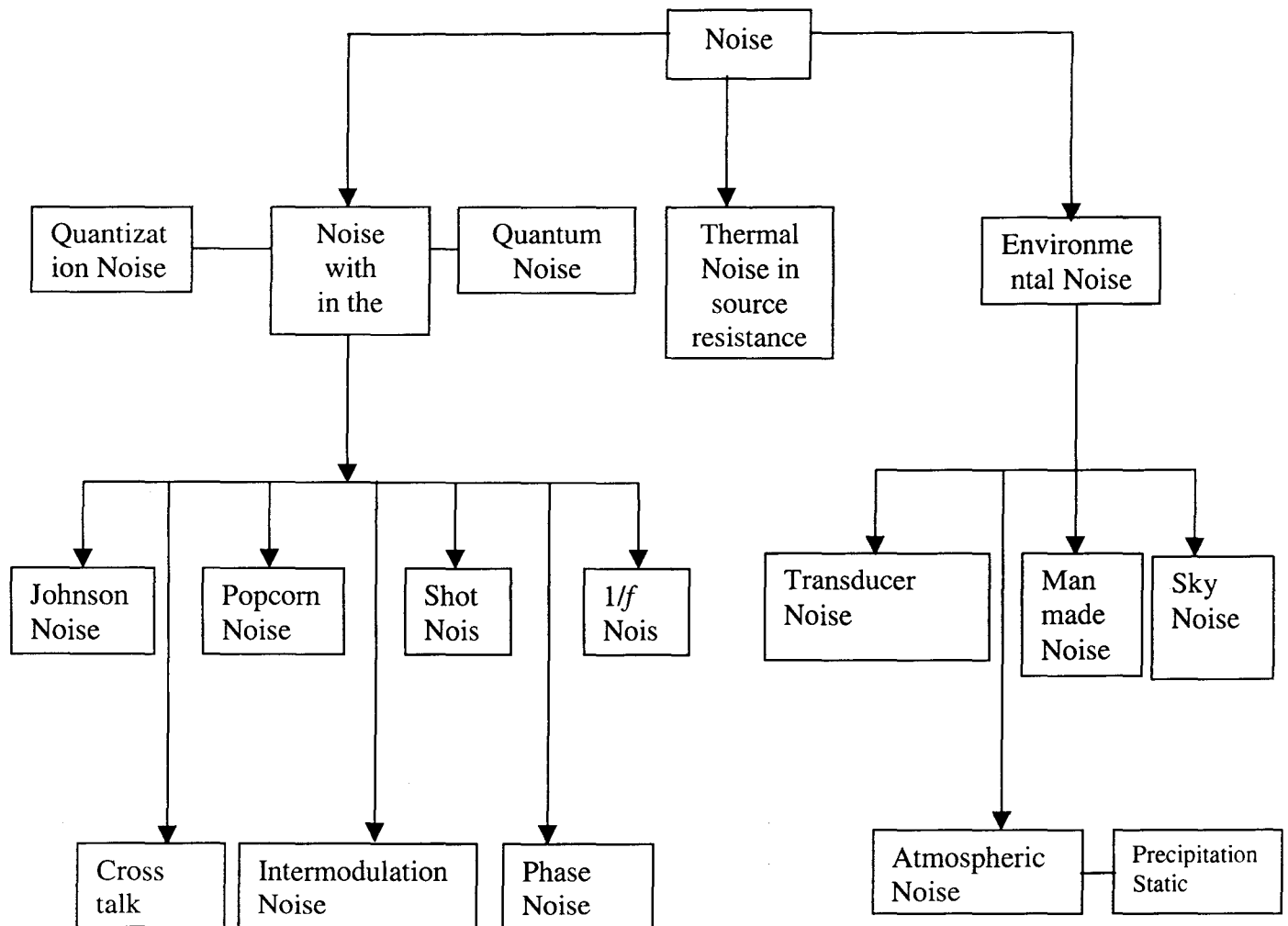


Fig 1.1 Principle sources of noises

Thermal noise

Thermal noise is the result of the random motion of charged particles (usually electrons) in a conducting medium such as a resistor due to the thermal agitation. Since all circuits necessarily contain resistive devices, thermal noise sources appear throughout all electrical circuits. The power spectrum of thermal noise is quite wide and is essentially uniform over the RF spectrum of interest for most communications applications.

In basic circuit theory, a resistance is considered as a passive device containing no energy. In reality, however, all resistive devices generate a small level of thermal noise as a result of the random motions of the electrons within the device. This effect is usually insignificant in applications where the signal levels are moderate to large. However, in communication systems, signal levels at the antenna and within the first few stages of a receiver are often of the order of microvolts. In this case Thermal noise may completely overshadow a small signal and render it completely unintelligible. . This noise is also referred to as Johnson or White or Nyquist noise.

Consider a resistor of resistance R at a physical temperature T °K (Refer Fig 1.1). Let E_n represent the rms thermal Noise voltage appearing across it at any instant of time. It is related to the noise bandwidth, its physical temperature and its resistance in a way given by Eq.1.1. It can be reduced by cooling.

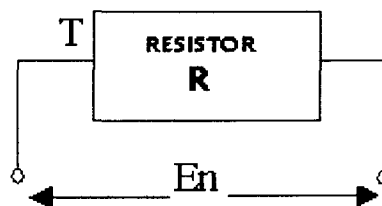


Fig 1.2 Resistor R at a physical temperature T °K

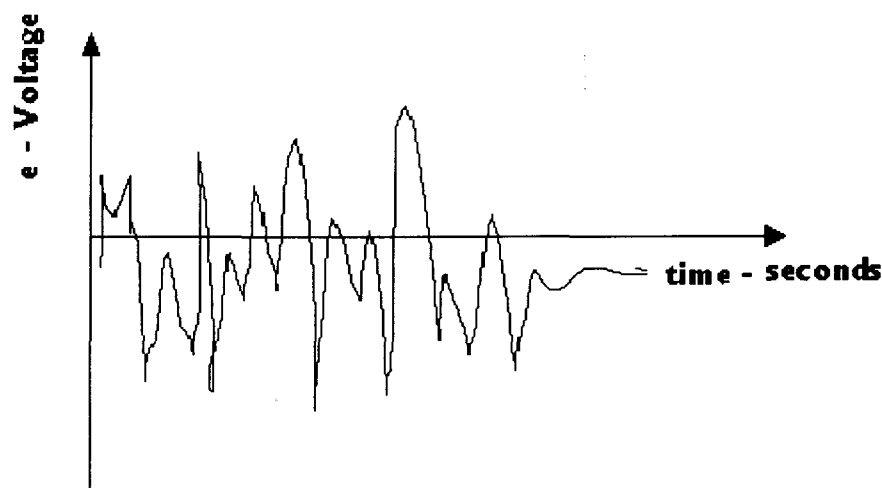


Fig 1.3 Characteristics of Thermal noise voltage.

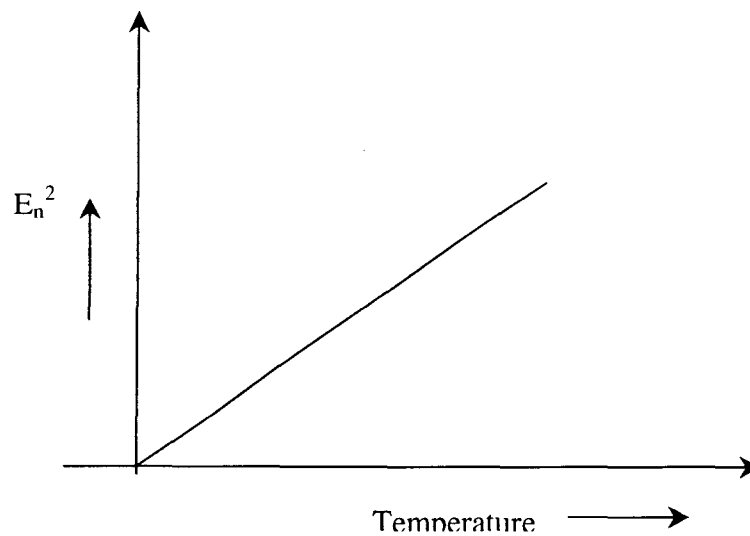


Fig 1.4 Variation of the thermal power with temperature

$$E_n = \sqrt{4RKT B_n} \quad 1.1$$

Where R is Resistance of the conductor, ohms

T is Conductor temperature, Kelvin

B_n is Noise bandwidth, Hz

K is Boltzmann's constant = 1.38×10^{-23} J / °K

Shot Noise

Shot noise arises from the discrete nature of current flow in electronic devices such as transistors and tubes. There will be a random variation in the number of electrons or holes crossing the semiconductor junction, this gives rise to a random fluctuation of current (Refer Figs 1.4 and 1.5). The associated random variation in the current appears as a disturbance to the signal being processed by the device, and so the result is a form of noise. The power spectrum of shot noise is similar to that of thermal noise, and the two effects are usually lumped together for system analysis. Although it is always present, it is not observed during the measurement because it is small compared to the DC value. However, it does contribute significantly to the noise in the amplifier circuit.

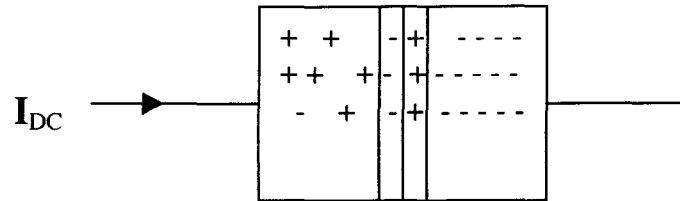


Fig 1.5

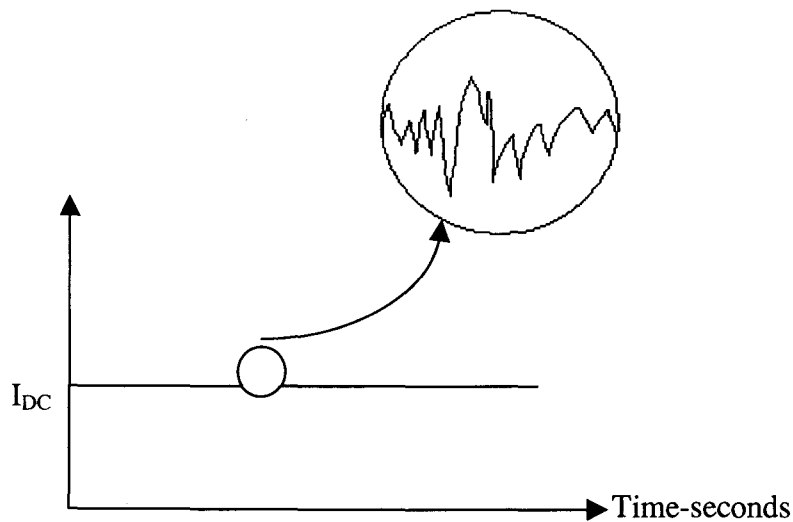


Fig 1.6 Superposition of shot noise current over DC

The rms shot noise current is related to the Noise bandwidth and the direct current in a way given by Eq.1.2

$$I_n = \sqrt{2 I_{dc} q_e B_n} \quad 1.2$$

Where I_{dc} is the mean direct current in amperes and

q_e is the magnitude of electron charge = $1.6 \times 10^{-19}C$

Shot noise is the current dependent effect, and the shot noise is directly proportional to the mean direct current.

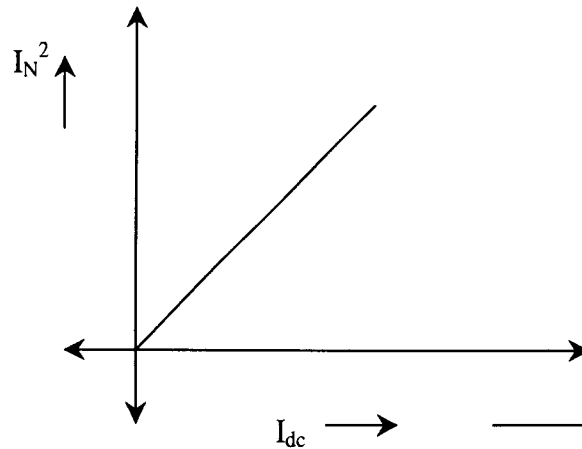


Fig 1.7 Variation of signal power to mean DC current

Flicker Noise

Flicker noise (also called $1/f$ noise) is a somewhat vaguely understood form of noise occurring in active devices such as transistors at very low frequencies. This noise arises from the fluctuation in the carrier densities in a semiconducting material. This gives rise to fluctuations in the conductivity of the material. It is most significant near dc and a few hertz and is usually negligible above about 1 kHz or so. Flicker noise is often a limiting factor for the minimum signal level that can be processed by a direct-coupled (dc) amplifier. The spectral density of this noise increases as frequency decreases.

Generation – Recombination Noise

For Semiconductor devices this noise is often defined as the noise produced by the random generation and recombination of electron – hole pairs.

Diffusion Noise

Since diffusion is a random process, fluctuations in the diffusion rate produce localized fluctuations in the carrier density. Such spontaneous fluctuations are called "Diffusion Noise". Diffusion noise is a more general process than the thermal noise.

Modulation Noise

This refers to noise not directly caused by fluctuations in the transition or diffusion rate. Instead this is due to fluctuations in carrier density or current flow produced by some modulation techniques.

Partition Noise

Partition noise occurs whenever current has to divide between two or more electrodes. It is due to the random fluctuations in the division. It has got flat Noise spectrum.

1.2 Basic definitions

Signal-to-Noise-Ratio:

It is defined as a relative measure of the desired signal power to the noise signal power. The S/N ratio is often designated simply as S/N and can be expressed as

$$S/N = \frac{\text{desired signal power}}{\text{noise signal power}} = \frac{P_s}{P_N} \quad 1.3$$

Where P_s = Signal power

P_n = Noise Power

V_s = Signal voltage

V_n = Noise voltage.

It can be expressed in decibel form as

$$S/N = 10 \log_{10} (P_s / P_N)$$

Noise figure:

The Noise figure F describes the quantity of a noisy microwave amplifier. It is defined as the ratio of total available noise power at the input to the total available at the output due to the thermal noise alone. Therefore it can be expressed as

$$F = \frac{P_o}{G P_{inTh}} \quad 1.4$$

It can also be expressed as the ratio of the signal- to- noise power ratio at the input to the signal - to - noise power at the output

$$F = \frac{P_{Si} / P_{Ni}}{P_{So} / P_{No}} \quad 1.5$$

Noise temperature:

Normally the noise power is expressed in terms of temperature. This temperature is the temperature of a fictitious resistor which will produce the same amount of thermal noise power as that of a thermal noise source.

The noise temperature is given as

$$T_E = (F - 1) T_o \quad 1.6$$

Where $T_E =$ noise temperature in deg Kelvin

$F =$ noise factor

$T_o =$ ambient temperature.

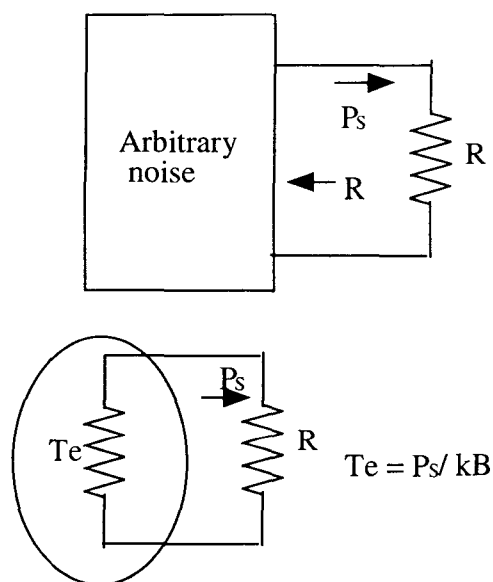


Fig 1.8 The equivalent noise temperature T_e , of an arbitrary noise source

1.3 General receiver configuration in a Radio Telescope

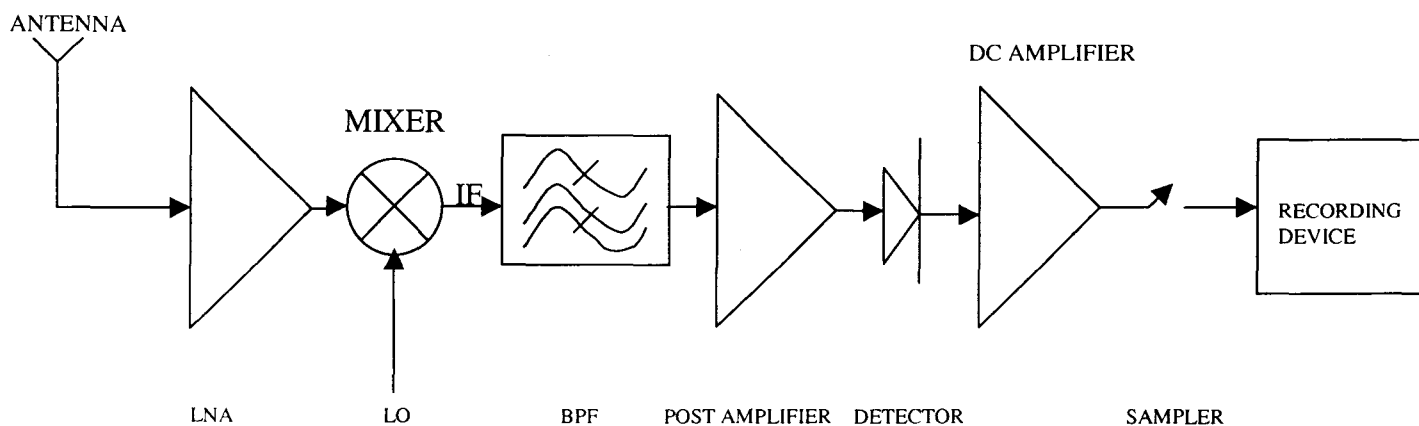


Fig.1.9 General Receiver configuration in a Radio Telescope

The above Fig shows a typical receiver setup of a Radio Telescope. The received signal from the antenna is amplified using the Low Noise Amplifier and down converted using a mixer. The IF signal obtained is band limited to reject any unwanted signal and is further amplified using a post amplifier. The output from the post amplifier is fed to the detector circuit produces a DC output proportional to the input RF power. The detected signal is further amplified using DC amplifier, digitized and stored in a computer for offline analysis.

1.3.1 Importance of Low Noise Amplifier in the Radio Receiver

As we see from Fig.1.5 the receiver consists of a number of RF devices and each one of them contributes its own noise. The major noise contribution comes from the very first stage. The noise contribution of the subsequent stages will be very small only when the gain of the first stage amplifier is large. This follows from Friis formula for overall Noise factor of amplifiers in cascade.

$$F = F_1 + \frac{F_2 - 1}{G_1} + \frac{F_3 - 1}{G_1 G_2} + \dots + \frac{F_i - 1}{G_1 G_2 \dots G_i} \quad 1.7$$

Where F is overall Noise factor

F_i & G_i are the Noise factor and the gain of the i^{th} stage amplifier. Since the first stage in the receiver is an amplifier the Noise contribution of it must be made as low as possible. In general the quality of any Radio receiver is decided by the noise performance of the first stage amplifier.

2. DEVICE THEORY

2.1 Basic definitions

Electron Mobility: It is defined as the ratio of electron drift velocity to the electric field.

$$\mu = V_d / E \quad 2.1$$

where, μ = Electron mobility($\text{cm}^2/\text{V- Sec}$)

V_d = Electron drift velocity (cm/Sec)

E = Applied electric field (volt/cm)

Transconductance: It is the ratio of change in the output current to the change in the input voltage.

$$g_m = \Delta I_{ds} / \Delta V_{gs} \quad 2.2$$

ΔI_{ds} = Change in output current

ΔV_{gs} = Change in input voltage

Cutoff frequency (f_T): It is the frequency at which the short circuit gain is approximately equal to unity.

$$f_t = g_m / (2\pi C_{gs})$$

where, g_m is the transconductance

C_{gs} is the gate-source capacitance

2.2 Active devices

Several solid state devices have been developed for use in the RF/Microwave circuits for various applications. They include silicon BJT's, silicon metal oxide semiconductor FET (MOSFET's), laterally diffused metal oxide semiconductor (LDMOS) transistors, GaAs metal semiconductor field effect transistor (MESFET's) or simply FET's, High electron mobility transistor (HEMT's) based on GaAs and InP and heterojunction bipolar transistors (HBT's) based on silicon germanium (SiGe) and GaAs.

Different applications require devices having different characteristics. For example, low noise amplifiers require transistors having low noise characteristics. Various substrate materials used for active devices are Silicon, Silicon Carbide, GaAs, InP and GaN. Table 2.1 below shows the electrical and physical properties of various semiconductor materials.

Table 2.1 Electrical and physical properties of various semiconducting materials

Property	Silicon	SiC	GaAs	InP	GaN
Semi-insulating	No	Yes	Yes	Yes	Yes
Resistivity (Ω -cm)	$10^3 - 10^5$	$>10^{10}$	$10^7 - 10^9$	$\sim 10^7$	$>10^{10}$
Dielectric constant	11.7	40	12.9	14	8.9
Electron mobility ($\text{cm}^2/\text{V-sec}$)	1450	500	8500	6000	800
Saturation velocity (cm/sec)	9×10^6	2×10^7	1.3×10^7	1.9×10^7	2.3×10^7
Radiation hardness	Poor	Excellent	Very good	Good	Excellent
Density (g/cm^3)	2.3	3.1	5.3	4.8	---
Thermal conductivity ($\text{W/cm}^\circ\text{C}$)	1.45	4.3	0.46	0.68	1.3
Operating temperature ($^\circ\text{C}$)	250	>500	350	300	>500
Energy gap (eV)	1.12	2.86	1.42	1.34	3.39
Breakdown field (kV/cm)	~ 300	≥ 2000	400	500	>5000

From the above table, the following points can be inferred:

- GaAs substrate has semi-insulating property. Hence, it offers lower insertion loss when compared to silicon.
- GaAs has higher mobility than silicon, hence it is used for manufacturing transistors having low noise characteristics.
- GaAs has high saturation velocity than silicon.

$g_m \propto v_s$, where g_m is the transconductance and v_s is the saturation velocity. Higher value of v_s results in higher value of g_m . This in turn results in the lesser noise of the device. Higher v_s also results in higher frequency band of operation.

- GaAs devices have higher cut off frequency compared to silicon devices.

This is because the cutoff frequency f_T , is directly proportional to the saturation velocity v_s and the saturation velocity of GaAs substrate is higher than silicon.

- GaAs substrate has high operating temperature than silicon.

2.3 Description of various devices

2.3.1 Microwave bipolar transistor

Fig 2.1 below illustrates a n-p-n transistor, properly biased as an amplifier. The three terminals are the emitter, base, and collector marked e, b, and c, respectively.

The input side of the transistor is forward biased, resulting in the injection of holes into the emitter n-type material and the injection of electrons into the p-type material of the base. Changes in the emitter current due to the signal E_g result in changes in the collector current I_c , but the net power into the load resistance R_1 will be a power gain over that in the input circuit.

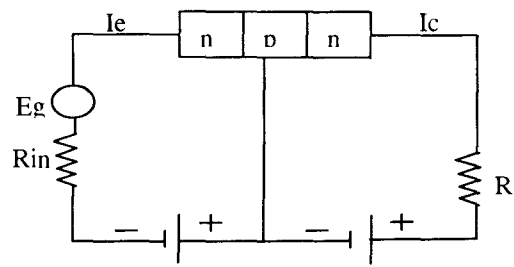


Fig 2.1 n-p-n Transistor Amplifier

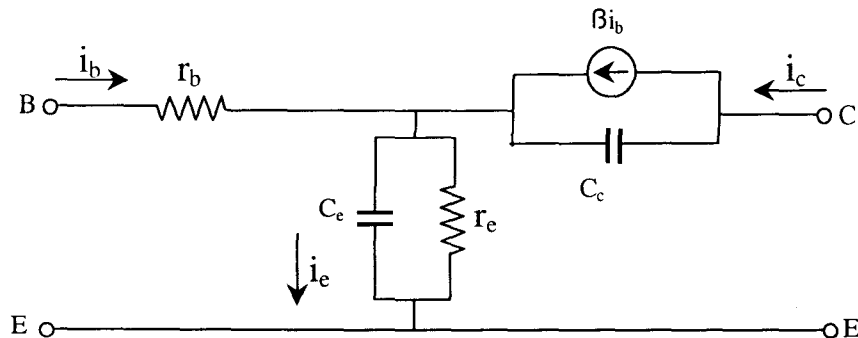


Fig 2.2 Equivalent Circuit of BJT

The equivalent circuit of the BJT is as shown in the fig 2.2. C_e and C_c corresponds to emitter-base capacitance and collector-base capacitance respectively. r_b and r_e represents the series resistance of base and emitter respectively.

The cutoff frequency of a charge-control type of microwave transistor is given by,

$$f_T = 1 / (2 \pi \tau) \quad 2.3$$

Where, τ is the transit time of the charge carriers

Typically the value of $\tau = 23$ pico sec hence calculated value of f_T is 6.9 GHz.

The high frequency response of microwave bipolar transistor is limited by the transit time of charge carriers across the base region. Attempt at reducing the width of the base region in order to decrease the transit time produces additional problems, i.e., increased capacitance and decreased tolerance to reverse bias potentials.

2.3.2 Field effect transistor

The structure of field effect transistor is shown in Fig.2.3. The voltage applied to the third terminal, the gate, controls the current flowing between the source and the drain. Also since the electron mobility is greater than the hole mobility, n-channel devices are considered.

The current flows from source to drain through the channel. The resistance of the channel is controlled by varying the width of the channel, through the gate voltage. With $V_g < 0$, the depletion region would further grow in to the channel narrowing the path for electrons to flow and thereby increasing the resistance of the channel. The voltage at which the whole channel is depleted of charge carriers is referred to as the pinch off voltage (V_p).

When a positive voltage is applied to the drain, the electric field across the channel would increase, and so would the velocity of the electrons. The voltage distribution across the channel would cause the difference in voltage between the gate electrode and the channel along the channel length. This would result in the different depth of the depletion region along the channel, which would increase toward the drain, as shown in Fig.2.2. Further increasing the drain voltage would cause the channel pinch-off .

Increasing the drain voltage beyond this voltage won't change the current much, since the pinch-off point would move toward the source and the voltage would drop across the depletion region. Increasing the gate voltage would decrease the depth of the depletion region into the channel. This will reduce the resistance of the channel.

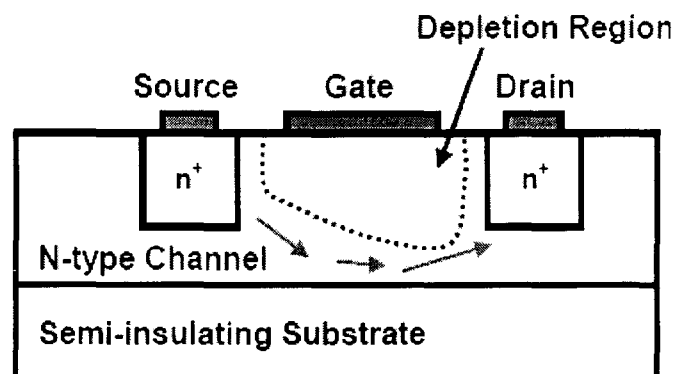


Fig 2.3 The schematic of field effect transistor

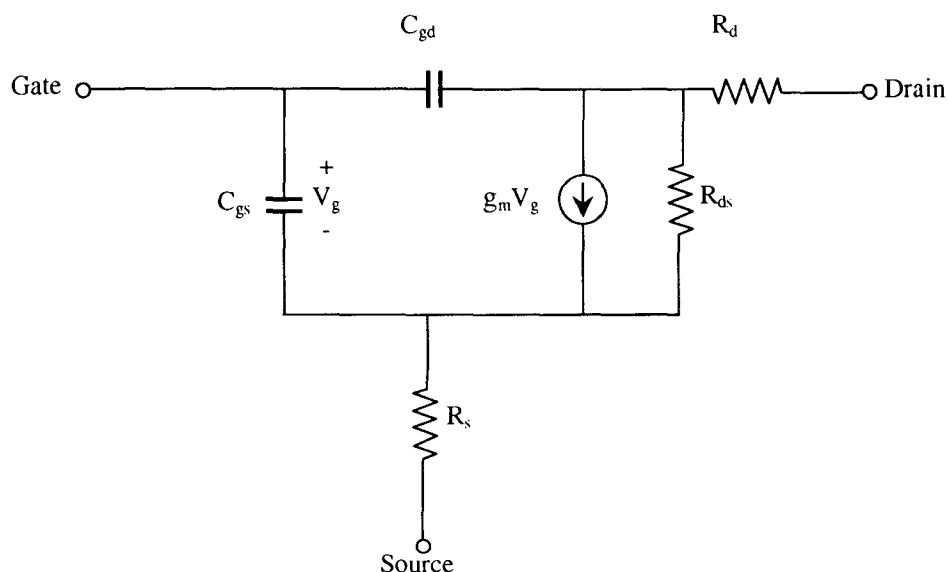


Fig 2.4 Equivalent Circuit of FET

Equivalent circuit of the FET is shown in fig 2.4. g_m represents the transconductance. C_{gd} and C_{gs} represents the gate-drain and gate-source capacitances respectively. Parasitic resistances, R_s and R_d depend upon the fabrication technology. R_{ds} represents the channel resistance.

Typically the value of τ is 7.69 picoseconds. Hence, the value of f_T is found to be 20 GHz.

Advantages of FET over the bipolar junction transistors are:

1. It has very high input resistance (Several Mega Ohms).
2. It has lower Noise Figure and thus is an improved pre-amplifier device.
3. It can have both voltage gain and current gain.

2.3.3 GaAs MESFET

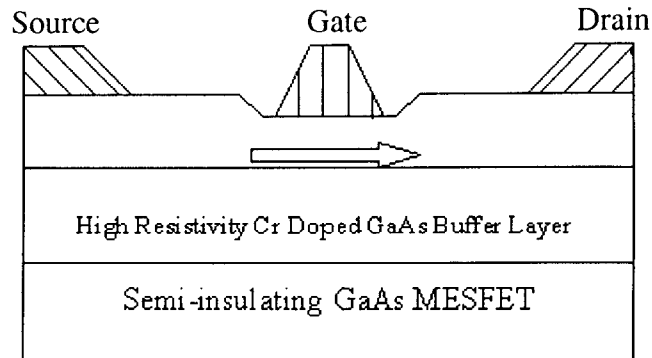


Fig 2.5 Structure of GaAs MESFET

The structure of the GaAs MESFET is as shown in the fig 2.5.

The source is maintained at ground potential and the drain at $+V_{DS}$, then the electron flow is from source to drain. A negative voltage $-V_{GS}$ reverse biases the rectifying metal semi-conductor gate junction, producing a depletion layer that controls the depth of the conducting channel. This modulation of the channel current consumes little power, since current into the reverse biased gate junction is small.

Fig.2.6 shows a voltage V_{ds} applied across the source and drain and another voltage V_{gs} applied across the source and gate of the MESFET. Within the channel under the gate, a region near the drain (x_1) is at a higher potential than x_0 . So the reverse bias and the depletion layer width are greater at x_1 than at x_0 . Since the channel is narrowing, the electric field E and electron drift velocity ' v ' must increase from x_0 to x_1 to maintain current. As V_{ds} is increased, the channel reverse bias increases and the depletion depth at x_1 extends nearly to the bottom of the channel. At this point, the channel is said to be pinched-off, and the current increases slowly with increasing V_{ds} . This leads to the familiar DC characteristics shown in the Fig 2.7

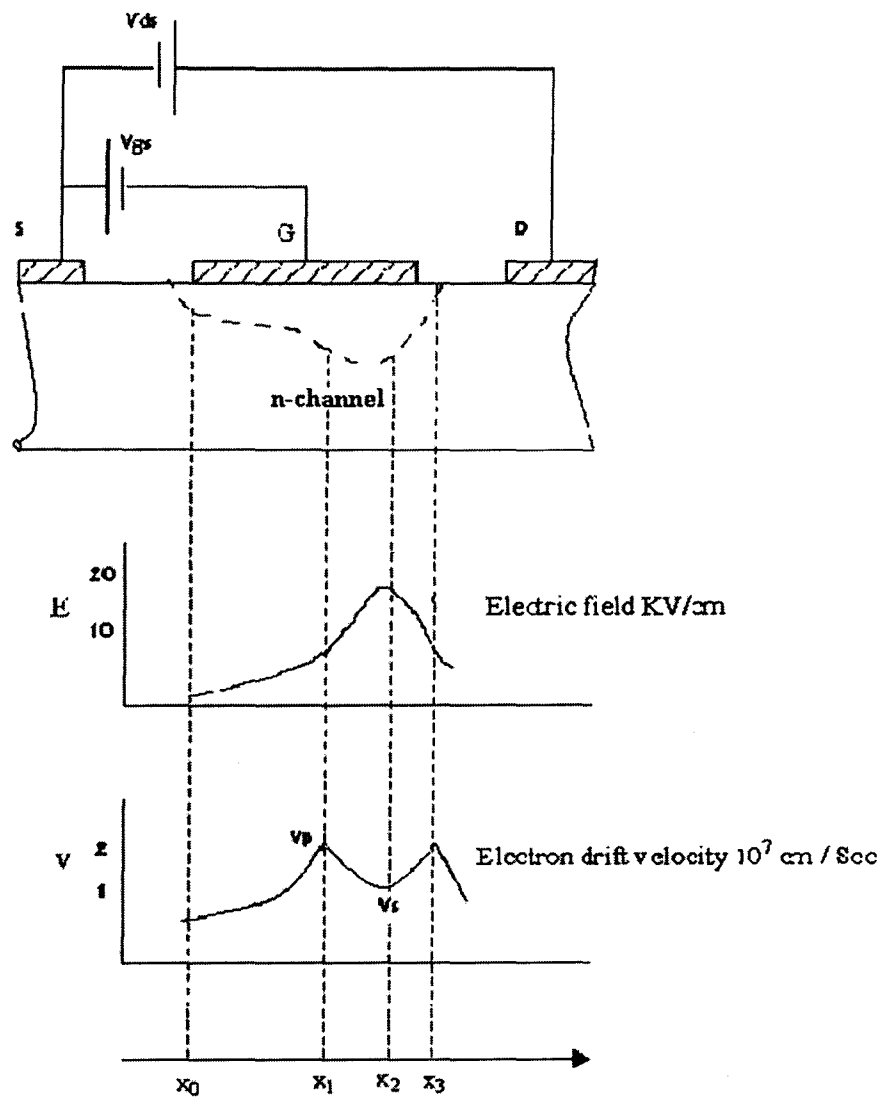


Fig 2.6 Physical conditions in a short gate FETs

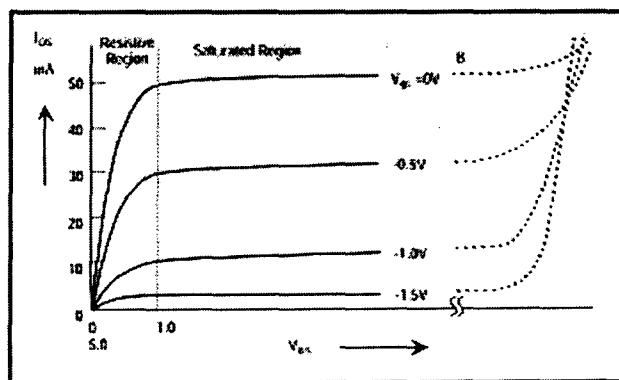


Fig 2.7 DC characteristics of GaAs MESFET

2.3.3.1 Equivalent Circuit Of GaAs MESFET

The small signal equivalent circuit of a GaAs FET in a common source configuration is as shown in fig 2.8

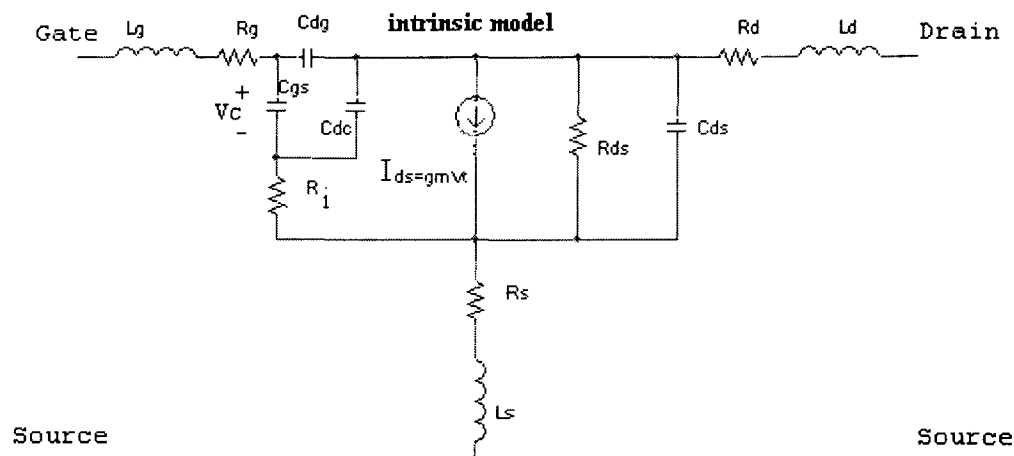


Fig 2.8 Equivalent circuit of GaAs FET

C_{gs} is the gate to source capacitance and C_{dg} is the drain to gate capacitance. C_{dc} is the gate to channel capacitance & C_{ds} the parasitic substrate capacitance. R_i & R_{ds} represent the effects of channel resistance, I_{ds} embodies the gain mechanism in a current source controlled by the voltage V_c via a transconductance g_m . The resistances R_s , R_g & R_d are strongly dependent on processing technology & affect microwave noise performance. Parasitic inductances L_s , L_g & L_d are associated with bonding wires that contact the transistor chip to the external circuit or to the package.

TRANSCONDUCTANCE vs DRAIN CURRENT

The transconductance is defined as

$$g_m = \frac{\Delta I_{ds}}{\Delta V_{gs}} \quad V_{ds} \text{ constant}$$

and has the units in Siemens. The value of the transconductance is dependent on the bias point. Fig. 2.9 shows g_m (transconductance) dependent on V_{gs} and hence on I_{ds} . The transconductance g_m , is dependent on the material carrier concentration profile characteristics. This curve signifies that the device gain, which is g_m dependent, will reduce with reducing I_{ds} .

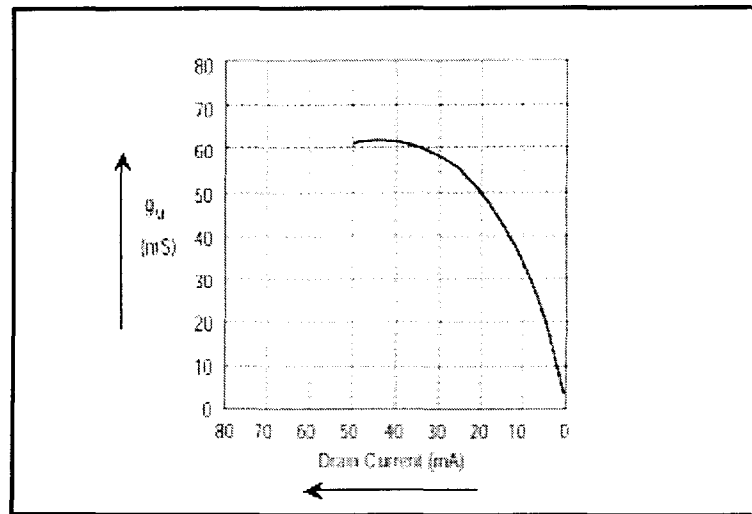


Fig 2.9 Transconductance (g_m) vs drain current

With increasing temperature the GaAs MESFET exhibits reducing I_{ds} , remaining thermally stable, unlike silicon where thermal runaway occurs. This is particularly important since GaAs has poor thermal conductivities compared to silicon.

2.3.3.2 Figures of merit of GaAs MESFET

In general, above 2GHz the silicon bipolar performance is unacceptable, as an amplifier device. However, in some applications such as oscillators, the lower $1/f$ noise of the silicon devices can still be used to advantage. For silicon a $1/f$ frequency of 1MHz compares with 10MHz for GaAs. Below 2GHz the choice of silicon bipolar or GaAs MESFETs is application dependent. At microwave frequencies the GaAs MESFET is invariably used on the common source configuration to provide the highest gain.

A number of figures of merit are defined for the GaAs MESFETs.

- a) The cut-off frequency, f_t , is the frequency at which we have unity current gain, i.e. the rf current through C_{gs} is equal to the output current, where output current is defined by the current generator g_m , is given by the equation below. It can also be expressed in terms of V_s and L , where V_s represents saturation velocity and L represents the effective gate length.

$$f_t = \frac{g_m}{2\pi C_{gs}} = \frac{V_s}{2L}$$

- b) The maximum frequency of oscillation. F_{max} , is a more meaningful figure of merit, defined as the frequency where the power gain is unity. This is clearly greater than f_t .

$$f_{max} = \frac{f_t}{2} (g_m R_{ds})$$

The typical value of τ is 1.25 picosecond. The calculated value of the cutoff frequency = 127 GHz . hence GaAs MESFETs are preferred at higher frequencies.

2.3.3.3 Different types of Noise in FETs

The sources of noise in FET can be broadly classified in to two Intrinsic noise sources and Extrinsic noise sources

(i) Intrinsic noise sources:

The noise sources intrinsic to the FET are thermal noise in channel and gate induced noise. The gate induced noise source is highly correlated with the noise generated in the channel since any fluctuation in the channel will induce a voltage at the gate. They primarily depend on the bias conditions.

(ii) Extrinsic Noise Sources:

The resistances associated with the FET, namely the gate metallization resistance R_g , the source resistance R_s and gate bonding resistance produce thermal noise within them. They form the major extrinsic sources of noise.

2.3.4 High electron mobility transistor

A high electron-mobility transistor (HEMT), based on a modulation-doped GaAs-AlGaAs single heterojunction structure, was developed by Fujitsu of Tokyo in the year 1979.

In HEMT the density of the doping species is modulated so as to confine and control a two-dimensional electron gas. Its frequency of operation is very high and is of

the order of few tens of GHz. The HEMT offer low noise when compared to the GaAs MESFETs due to the high electron mobility in the device channel. The frequency of operation is also increased due to the same reason. The major improvements over MESFETs include shorter gate lengths, reduced gate and source contact resistances, and optimized doping profiles.

In a Heterostructure Field Effect Transistor (HFET), a wide band gap semiconductor separates the gate electrode from the active channel. A High Electron Mobility Transistor (HEMT) as a HFET device consists of several layers of compound semiconductor as shown in fig 2.10. An active channel is formed at the interface of the buffer layer of GaAs and the doped, wide band gap material, such as AlGaAs. The donor layer of n-AlGaAs supplies the electrons for the channel conduction. These are the free electrons and they are allowed to move in the lattice and will fall in the lowest energy state, which is available at the GaAs side of the hetero-junction. Since the undoped GaAs and AlGaAs have different band gap energies, as shown in the fig. 2.11, the electron flow is confined to the interface between these two layers. Thus all these electrons are accumulated in the junction between these two layers forming a small layer of free electrons in the channel as shown in the figure 2.10. The thickness of this layer is about 100 \AA , which is much smaller than Broglie wavelength of the electrons. Hence the electrons present in that layer are quantized in a 2D system at the interface of the hetero-junction, i.e. they are free to move only in the two directions and the layer is known as 2D Electron Gas (2DEG) as shown in figure 2.10. As the electrons are separated from the donor layer of n-AlGaAs, there will be less impurity scattering and therefore mobility and effective velocity of electrons for a certain electric field is very high.

This sheet of electrons with high mobility can be served as the channel of FET, and can be modulated through the gate voltage, i.e. the number of electrons in the 2DEG is modulated through the gate voltage.

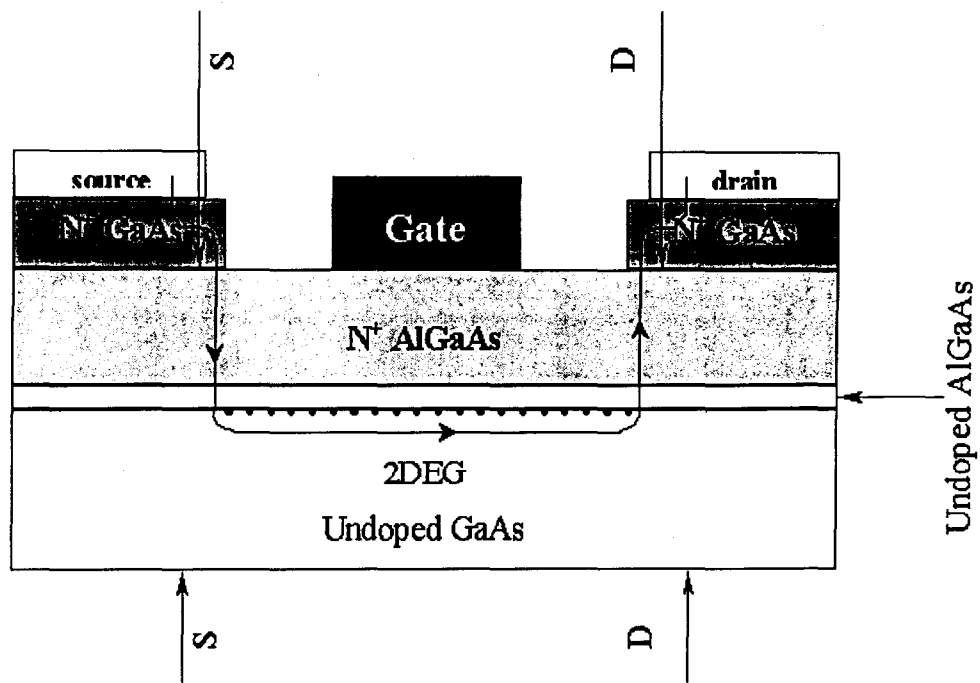


Fig 2.10 Structure of HEMT

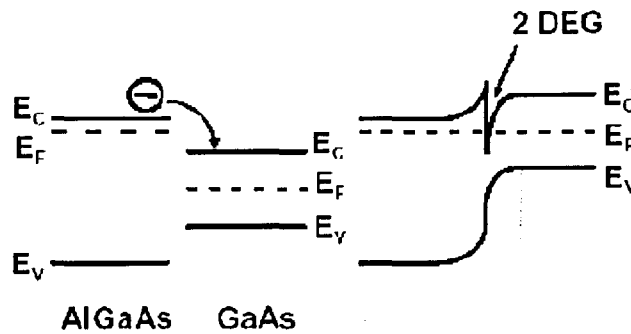


Fig 2.11 The energy band diagram of doped AlGaAs (wide band gap), GaAs (small band gap) and their hetero-structure and the formation of 2DEG.

Usually there is a undoped spacer layer with the thickness of about 20-60 Å, in between the buffer and the donor layer. This separates the donors and the electrons, which reduces the coulombic scattering caused by the electrical interaction between them. The thickness of this layer is set in way that both the saturation velocity and the mobility of electrons are maximized. Also in this structure a semi-insulating material is used as a substrate in order to have isolation between the adjacent devices

The operation of HEMT is different from MESFET. In the latter, the depletion region width is modulated by the input signal, there by modulating the channel current. In HEMT, however, the channel width is fairly constant. It is the number of electrons flowing, which are regulated or modulated by the input signal. In other words, modulation on charge flow is direct. The I-V characteristics of HEMT are as shown in Fig 2.12.

The typical value of τ is $.0769 \times 10^{-11}$ seconds. The cut off frequency of HEMT is calculated to be 2×10^{17} Hz. Hence HEMT is preferred at higher frequencies.

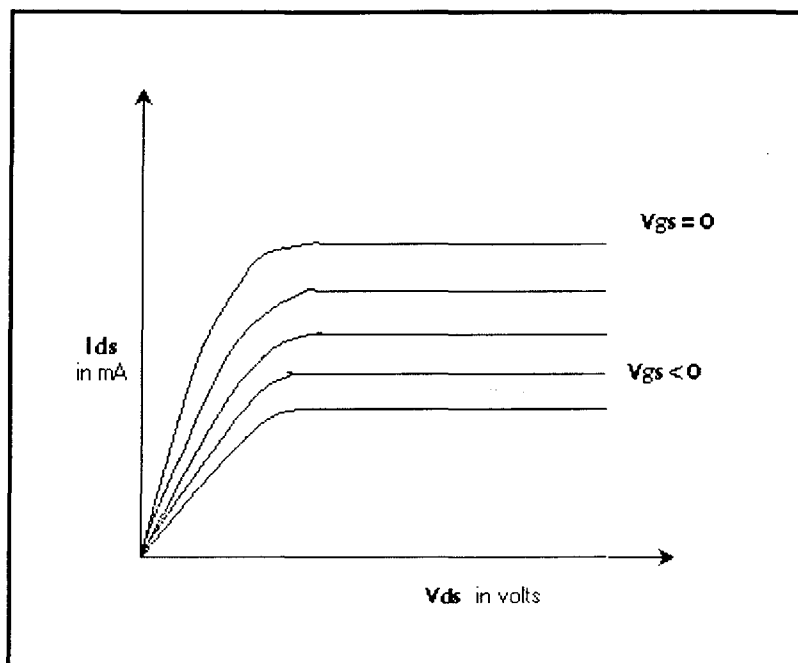


Fig:2.12 DC characteristics of HEMT

3. CIRCUIT THEORY

3.1 S-parameters

3.1.1 Introduction

From the network theory, we understand that any two-port network can be characterized by parameters like such as the H, Y and Z parameters.

For the network shown in the figure, the input and output parameters are defined in terms of these parameters as shown below,

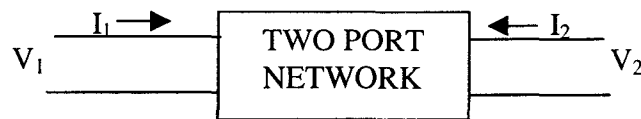


Fig 3.1

H-parameters

$$V_1 = h_{11}I_1 + h_{12}V_2$$

$$I_2 = h_{21}I_1 + h_{22}V_2$$

Y-parameters

$$I_1 = y_{11}V_1 + y_{12}V_2$$

$$I_2 = y_{21}V_1 + y_{22}V_2$$

Z-parameters

$$V_1 = z_{11}I_1 + z_{12}I_2$$

$$V_2 = z_{21}I_1 + z_{22}I_2$$

All these network parameters relate total voltages and total currents at each of the two ports.

For example $h_{11} = (V_1/I_1)$ when $V_2 = 0$ (applying short circuit to the output port) gives the input impedance of the network.

Similarly $h_{12} = (V_1/V_2)$ when $I_1 = 0$ (by open circuiting input port) gives the reverse voltage gain.

The important thing to note here that both open and the short circuit are essential for making these measurements.

If the frequencies are of microwave range, however, the H, Y and Z parameters cannot be measured because:

- 1) the physical length of the component or line will be comparable or much larger than the wavelength. Thus voltage and current are not defined at a given point.
- 2) short and open circuits are difficult to achieve over a broadband of frequencies.
- 3) active devices, such as transistors, frequently will not be short or open circuit stable, because at higher frequencies, short circuit looks like an inductor and an open circuit has some leakage capacitance and an active device will oscillate when terminated with a reactive load.

Consequently, some new method of characterization is needed to overcome these problems. The logical variables to use at the microwave frequency are traveling waves rather than total voltages and total currents.

3.1.2 S-parameters of a two-port network

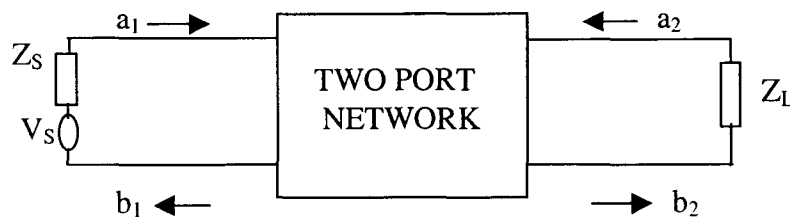


Fig 3.2

Figure shows a two-port network connected to a source V_s . a_1 and a_2 are the voltages incident and b_1 and b_2 are the voltages reflected.

Incident voltages and reflected voltages are related to each other through S-parameters as shown below,

$$\begin{aligned} b_1 &= S_{11}a_1 + S_{12}a_2 \\ b_2 &= S_{21}a_1 + S_{22}a_2 \end{aligned} \quad 3.1$$

where,

S_{11} =input reflection coefficient, when output is terminated in a matched load.

S_{22} =output reflection coefficient when input is match terminated.

S_{12} =reverse transmission coefficient.

S_{21} =forward transmission coefficient

$$S_{11} = (b_1 / a_1) | a_2 = 0$$

$$S_{22} = (b_2 / a_2) | a_1 = 0$$

$$S_{12} = (b_1 / a_2) | a_1 = 0$$

$$S_{21} = (b_2 / a_1) | a_2 = 0$$

The signal flow graph for the two-port under input-output mismatch is given by,

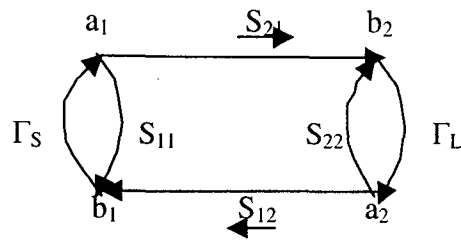


Fig 3.3

And the two-port network is represented as,

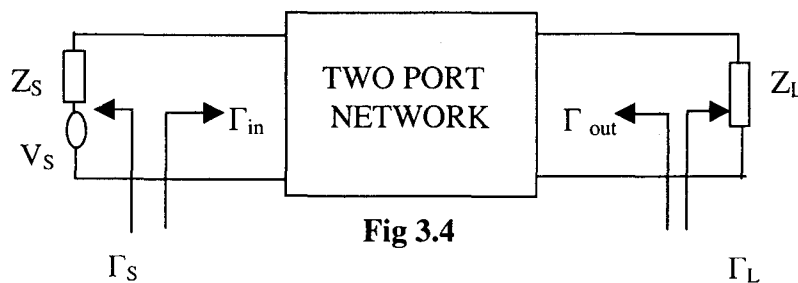


Fig 3.4

Under input-output matched conditions, the source reflection coefficient (Γ_S) and load reflection coefficient (Γ_L) are zero and hence flow graph is given by,

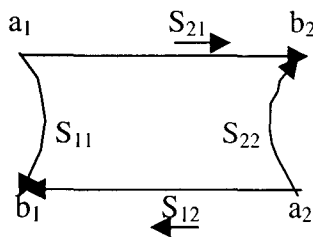


Fig 3.5

Hence, the input reflection coefficient (Γ_{in}) under mismatched load condition is given by,

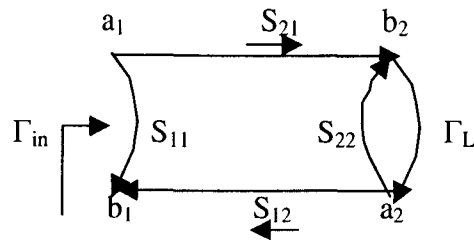


Fig 3.6

$$\Gamma_{in} = S_{11} + \frac{S_{12} \Gamma_L S_{21}}{1 - S_{22} \Gamma_L} \quad 3.2$$

Output reflection coefficient (Γ_{out}) under mismatched source condition is given by,

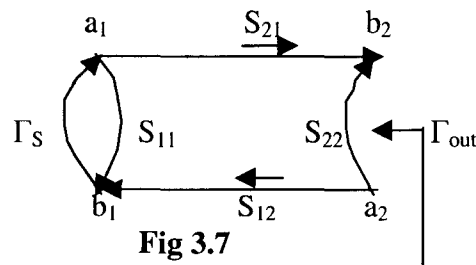


Fig 3.7

$$\Gamma_{out} = S_{22} + \frac{S_{12} \Gamma_S S_{21}}{1 - S_{11} \Gamma_S} \quad 3.3$$

3.2 Power gain equations

We define three types of power gains for an amplifier. These are as follows:

1) Transducer power gain (G_T)

$$G_T = (P_L / P_{AVS}) = (\text{power delivered to the load} / \text{power available from the source})$$

2) Operating power gain (G_P)

$$G_P = (P_L / P_{in}) = (\text{power delivered to the load} / \text{power input to the network})$$

3) Available power gain (G_A)

$$G_A = (P_{AVN} / P_{AVS}) = (\text{power available from the network} / \text{power available from the source})$$

The three power gains can be represented in equation form as

$$G_T = \frac{(1 - |\Gamma_S|^2)}{(1 - |\Gamma_{in}\Gamma_S|^2)} [|S_{21}|^2] \frac{(1 - |\Gamma_L|^2)}{(1 - |\Gamma_{out}\Gamma_L|^2)} \quad 3.4$$

$$G_P = \frac{1}{(1 - |\Gamma_{in}|^2)} [|S_{21}|^2] \frac{(1 - |\Gamma_L|^2)}{(1 - |S_{22}\Gamma_L|^2)} \quad 3.5$$

$$G_A = \frac{(1 - |\Gamma_S|^2)}{(1 - |S_{11}\Gamma_S|^2)} [|S_{21}|^2] \frac{1}{(1 - |\Gamma_{out}|^2)} \quad 3.6$$

3.3 Simultaneous conjugate matching

From equation 3.4, We understand the conditions required to obtain maximum transducer power gain (G_T) are

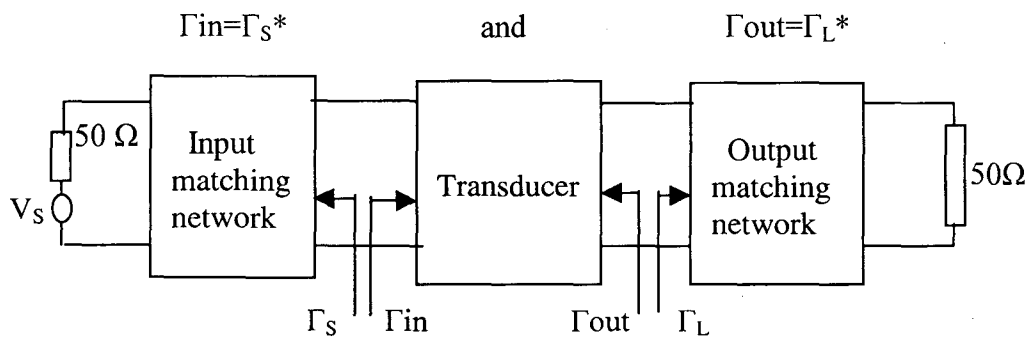


Fig 3.8

$$\text{Hence, } \Gamma_S^* = \Gamma_{in} = S_{11} + \frac{(S_{12} \Gamma_L S_{21})}{(1 - S_{22} \Gamma_L)} \quad 3.7$$

$$\Gamma_L^* = \Gamma_{out} = S_{22} + \frac{(S_{12} \Gamma_S S_{21})}{(1 - S_{11} \Gamma_S)} \quad 3.8$$

3.4 Stability circles and its importance

The stability of an amplifier or its resistance to oscillate is a very important consideration in the design and it can be determined from the S-parameters, matching networks and the terminations.

In a two-port network, oscillations are possible when either input or output port presents a negative resistance. This occurs when $|\Gamma_{IN}| > 1$ or $|\Gamma_{OUT}| > 1$. The two port network is said to be unconditionally stable at a given frequency if the real parts of Z_{IN} and Z_{OUT} are greater than zero for all passive loads and source impedances.

If the two-port is not unconditionally stable it is potentially unstable, that is, some passive load and source terminations can produce input and output impedances having a negative real part.

The conditions for unconditional stability are,

$$\begin{aligned}
 & |\Gamma_S| < 1 \\
 & |\Gamma_L| < 1 \\
 |\Gamma_{IN}| = & \left| S_{11} + \frac{S_{12} S_{21} \Gamma_L}{1 - S_{22} \Gamma_L} \right| < 1 \\
 |\Gamma_{OUT}| = & \left| S_{22} + \frac{S_{12} S_{21} \Gamma_S}{1 - S_{11} \Gamma_S} \right| < 1
 \end{aligned}$$

For a conditionally stable amplifier, the stability circles give the boundaries between the stable and unstable regions on the Smith chart.

The radii and centers of the circle where $|\Gamma_{IN}| = 1$ and $|\Gamma_{OUT}| = 1$ in the $|\Gamma_L|$ plane and $|\Gamma_S|$ planes respectively are given below

Γ_L values for $|\Gamma_{IN}| = 1$ (Output stability circle)

$$R_L = \left| \frac{S_{12} S_{21}}{|S_{22}|^2 - |\Delta|^2} \right| \quad (\text{radius})$$

$$C_L = \left| \frac{(S_{22} - \Delta S_{11}^*)^*}{|S_{22}|^2 - |\Delta|^2} \right| \quad (\text{centre})$$

$$\text{where } \Delta = |S_{11} S_{22} - S_{12} S_{21}|$$

Γ_S values for $|\Gamma_{OUT}|=1$ (input stability circle)

$$R_S = \left| \frac{S_{12} S_{21}}{|S_{11}|^2 - |\Delta|^2} \right| \quad (\text{radius})$$

$$C_S = \left| \frac{(S_{11} - \Delta S_{22}^*)^*}{|S_{11}|^2 - |\Delta|^2} \right| \quad (\text{centre})$$

For the device to be stable the input and output stability circles should lie outside the smith chart. Fig.3.9 shows typical input and output stability circles of an amplifier on the smith chart. The impedances offered by it both at the input and the output should not lie in the shaded regions as shown in the figure for stable operation.

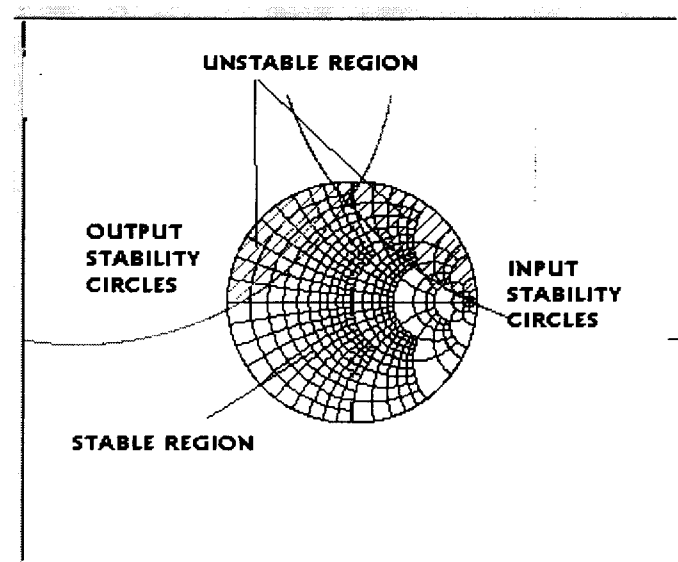


Fig 3.9 Smith chart showing input and output stability circles

A two-port network is said to be unconditionally stable provided the following necessary and sufficient condition is satisfied.

$$K = \frac{1 - |S_{11}|^2 - |S_{22}|^2 + |\Delta|^2}{2|S_{12}S_{21}|} > 1 \quad 3.9$$

$$\text{where } \Delta = |S_{11} S_{22} - S_{12} S_{21}| < 1 \quad 3.10$$

$K=1$ implies network is marginally stable and $K<1$ implies network is potentially unstable.

3.5 Constant gain circles

Practically, the gain obtained is always less than the maximum gain. This is because of the improper input and output matching sections which leads to a gain, less than maximum obtainable gain, in other words mismatches reduces the overall gain.

The gain design procedure of an amplifier is facilitated by plotting of constant gain circles on the smith chart, to represent loci of source reflection coefficient (Γ_s) and load reflection coefficient (Γ_L) that give fixed values of gain (G_s and G_L).

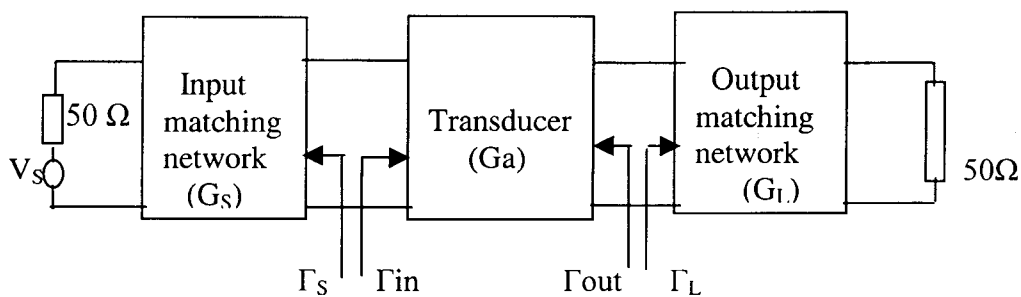


Fig 3.10

Since in the amplifier design S_{12} is almost negligible, so for finding out the gain circles for a unilateral condition, consider the expression of G_s and G_L for the unilateral network which are given as:

$$G_S = \frac{1 - |\Gamma_S|^2}{|1 - S_{11} \Gamma_S|^2} \quad 3.11$$

$$G_L = \frac{1 - |\Gamma_L|^2}{|1 - S_{22} \Gamma_L|^2} \quad 3.12$$

The gains are maximized when $\Gamma_S = S_{11}^*$ and $\Gamma_L = S_{22}^*$, resulting in maximum values given by,

$$G_{S_{\max}} = \frac{1}{1 - |S_{11}|^2} \quad 3.13$$

$$G_{L_{\max}} = \frac{1}{1 - |S_{22}|^2} \quad 3.14$$

Now we define the normalized gain factors g_S and g_L as,

$$g_S = G_S / G_{S_{\max}} = \frac{(1 - |\Gamma_S|^2)(1 - |S_{11}|^2)}{|1 - S_{11} \Gamma_S|^2} \quad 3.15$$

$$g_L = G_L / G_{L_{\max}} = \frac{(1 - |\Gamma_L|^2)(1 - |S_{22}|^2)}{|1 - S_{22} \Gamma_L|^2} \quad 3.16$$

Equation 3.15 is simplified to obtain,

$$|\Gamma_S - (g_S S_{11}^*) / [1 - (1 - g_S)|S_{11}^*|^2] = (1 - g_S)^{-1/2} (1 - |S_{11}|^2) / [1 - (1 - g_S)|S_{11}|^2]$$

Which is the equation of the circle with its centre and radius given by:

$$C_S = \frac{(g_S S_{11}^*)}{[1 - (1 - g_S)|S_{11}^*|^2]}$$

and

$$R_S = (1 - g_S)^{-1/2} (1 - |S_{11}|^2) / [1 - (1 - g_S)|S_{11}|^2] \quad \text{respectively.}$$

Similarly the constant gain circles for the output can be found out with:

$$C_L = (g_L S_{22}^*) / [1 - (1 - g_L) |S_{22}^*|^2] \quad \text{centre}$$

and

$$R_L = (1 - g_L)^{-1/2} (1 - |S_{22}^*|^2) / [1 - (1 - g_L) |S_{22}^*|^2] \quad \text{radius}$$

The gain circles can be plotted at a various frequencies with the S-parameters known and after plotting the gain circles on the smith chart, then Γ_S and Γ_L can be chosen along the circles to provide the required gains.

3.6 Noise model

A linear two port network containing no internal sources, can be represented by the open circuit impedance or short circuit admittance matrices,

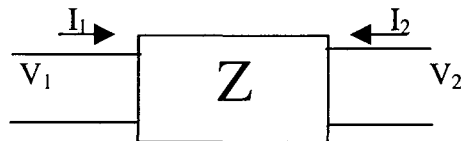


Fig 3.11

$$V_1 = Z_{11} I_1 + Z_{12} I_2$$

$$V_2 = Z_{21} I_1 + Z_{22} I_2$$

$$\begin{bmatrix} V_1 \\ V_2 \end{bmatrix} = \begin{bmatrix} Z_{11} & Z_{12} \\ Z_{21} & Z_{22} \end{bmatrix} \begin{bmatrix} I_1 \\ I_2 \end{bmatrix}$$

If the two port has internal sources, their effects are brought out to input and output terminals, following the thevenin's theorem. It is represented as shown,

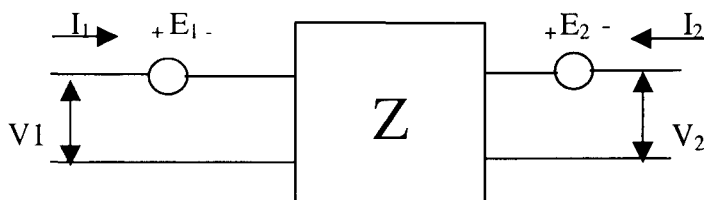


Fig 3.12

$$V_1 = Z_{11}I_1 + Z_{12}I_2 + E_1$$

$$V_2 = Z_{21}I_1 + Z_{22}I_2 + E_2$$

Note that the two equivalent generators E_1 and E_2 are not independent.

The two-port network having internal sources can also be represented as a combination of voltage and current generators using ABCD parameters.

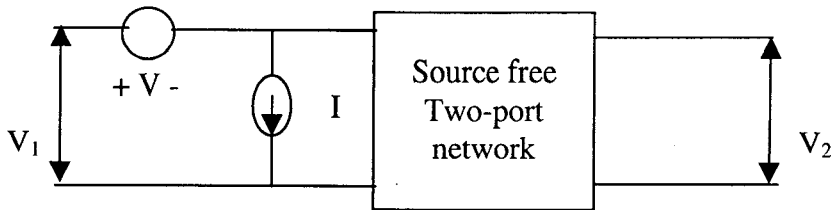


Fig 3.13

$$V_1 = AV_2 + BI_2 + V$$

$$I_1 = CV_2 + DI_2 + I$$

$$\begin{bmatrix} V_1 \\ I_1 \end{bmatrix} = \begin{bmatrix} A & B \\ C & D \end{bmatrix} \begin{bmatrix} V_2 \\ I_2 \end{bmatrix}$$

Note that V and I are not independent. Advantage of this representation is that the physical network can be split into two distinct parts, one containing the effects of all internal sources and the other one being completely passive. This is particularly useful when the internal sources are noise generators.

3.6.1 Application to noisy two port network

The two equivalent generators V and I become the noise generators e_n and i_n which are usually correlated to a degree.

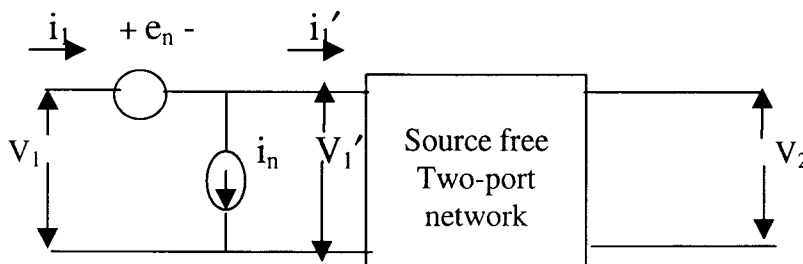


Fig 3.14

Either e_n or the i_n can be split into two parts – one fully correlated and the other uncorrelated.

Thus, let us consider series voltage generator e_n given by,

$$e_n = e_u + e(i)$$

where

e_u is the uncorrelated portion

$e(i)$ is the fully correlated portion

Since $e(i)$ is fully correlated with i_n , it is proportional to i_n .

Therefore, $e_n = e_u + i_n Z_c$ where in $Z_c = e(i)$ and $Z_c = R_c + jX_c$ (correlation impedance)

From the fig 3.14,

$$i_1 = i_n + i_1'$$

$$\text{Also, } V_1 = e_n + V_1'$$

$$V_1 = e_u + i_n Z_c + V_1'$$

Therefore

$$V_1 = e_u + Z_c (i_1 - i_1') + V_1'$$

The equation leads to the equivalent circuit shown below where both the correlation impedances Z_c and $-Z_c$ are noise free i.e. their noise temperature is 0°K .

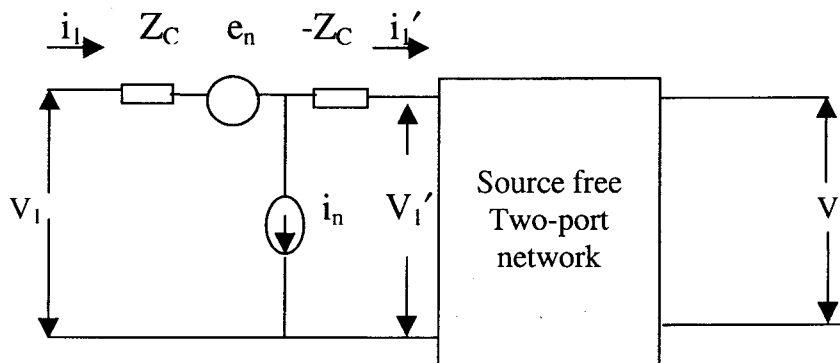


Fig 3.15

Now, e_u^2 and i_n^2 could be modeled as an equivalent resistance and conductance at reference temperature T_0 ,

$$\text{i.e. } e_u^2 = 4 K T_0 R_u df \quad \text{and}$$

$$i_n^2 = 4 K T_0 G_n df$$

Therefore noise equivalent circuit is given by

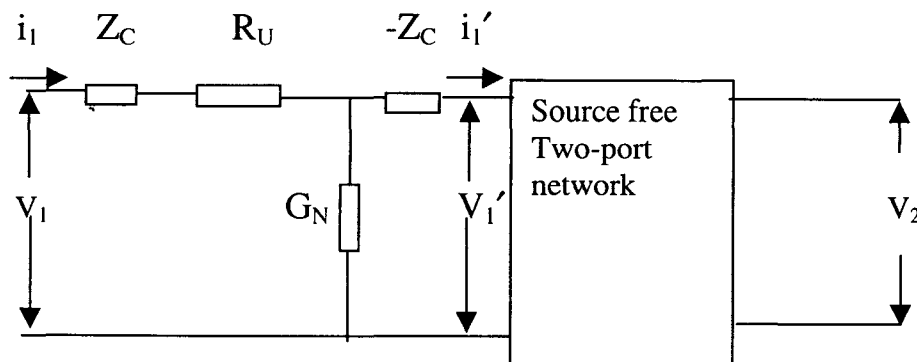


Fig 3.16

3.7 Dependence of noise factor on source admittance

We discuss the dependence of F on Y_g starting with the noise model developed earlier.

Consider the dual of the noise model,

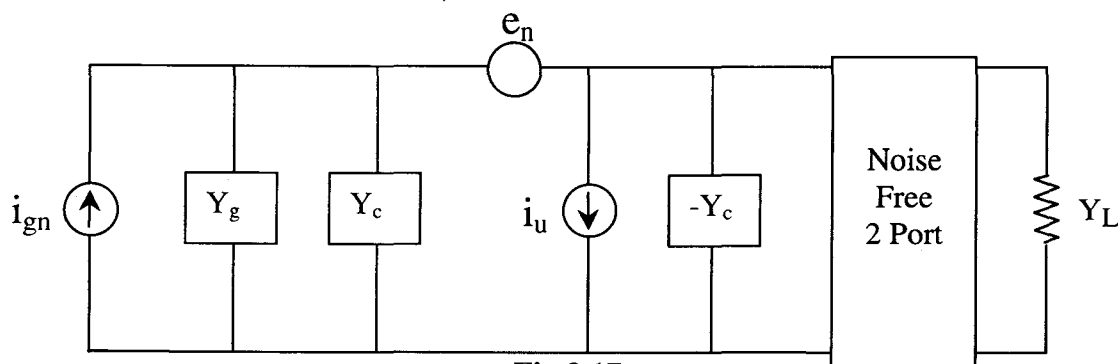


Fig 3.17

Now, we convert the series voltage generator e_n into an equivalent shunt current generator by applying Norton's theorem to the network comprised of e_n , Y_g and Y_c .

Thus,

$$i_n = e_n (Y_g + Y_c)$$

Therefore the noise model becomes,

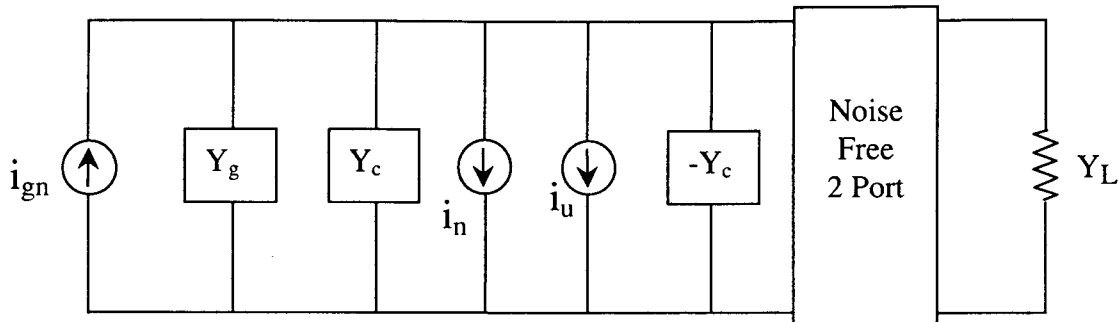


Fig 3.18

The noise factor F is given by,

$$F = \frac{\overline{i_{gn}^2} + \overline{i_n^2} + \overline{i_u^2}}{\overline{i_{gn}^2}} \quad 3.17$$

$$F = \frac{\overline{i_{gn}^2} + e_n^2 |Y_g + Y_c|^2 + \overline{i_u^2}}{\overline{i_{gn}^2}} \quad 3.18$$

$$F = \frac{4kT_0d_f G_g + 4kT_0d_f R_n^2 |Y_g + Y_c|^2 + 4kT_0d_f G_u}{4kT_0d_f G_g} \quad 3.19$$

Simplifying the above equation, we get

$$F = 1 + \frac{G_u}{G_g} + \frac{R_n [(G_g + G_c)^2 + (B_g + B_c)^2]}{G_g} \quad 3.20$$

To obtain minimum noise factor, we need to tune G_g to G_c and B_g to B_c .

Hence, we obtain the expression for F as,

$$F = F_{min} + \frac{R_n [(G_g + G_{g0})^2 + (B_g + B_{g0})^2]}{G_g}$$

$$F = F_{min} + \frac{R_n |Y_g - Y_0|^2}{G_g} \quad 3.21$$

Now, expressing Y_g and optimum admittance Y_0 in terms of reflection coefficients, we get,

$$Y_g = \frac{1 - \Gamma_S}{1 + \Gamma_S}$$

$$Y_0 = \frac{1 - \Gamma_0}{1 + \Gamma_0}$$

Hence,

$$F = F_{\min} + \frac{4 R_n |\Gamma_S - \Gamma_0|^2}{(1 - |\Gamma_S|^2)(1 + |\Gamma_0|^2)} \quad 3.22$$

Therefore, the noise parameters are Γ_0 , F_{\min} and R_n , which are specified by the manufacturer.

Hence, if we match Γ_S to Γ_0 , then $F = F_{\min}$ and we obtain minimum noise factor.

3.8 Noise figure circles

In a low noise amplifier design the first stage of a receiver front end has a dominant effect on the noise performance of the overall system. Generally it is not possible to obtain both minimum noise figure and maximum gain for an amplifier, so some sort of compromise must be made. This can be done with circles of constant noise figure to select the usable trade off between the noise figure and the gain.

To obtain the constant noise figure circles, consider the equation for minimum noise figure as given by equation 3.21,

$$F = F_{\min} + \frac{R_N |Y_S - Y_{\text{opt}}|^2}{G_S} \quad 3.23$$

Where the following definitions are applied,

$Y_S = G_S + jB_S$ = source admittance presented to the transistor.

Y_{opt} = optimum source admittance that results in minimum noise figure.

F_{\min} = minimum noise figure of the transistor, attained when $Y_S = Y_{\text{opt}}$

R_N = equivalent noise resistance of the transistor

G_S = real part of source admittance.

Expressing the Y_S and Y_{opt} in terms of Γ_S and Γ_{opt} as

$$Y_S = (1/Z_0) [(1 - \Gamma_S) / (1 + \Gamma_S)] \quad 3.24$$

$$Y_{opt} = (1/Z_0) [(1 - \Gamma_{opt}) / (1 + \Gamma_{opt})] \quad 3.25$$

From the above equations, we have

$$|Y_S - Y_{opt}|^2 = (4/Z_0^2) (|\Gamma_S - \Gamma_{opt}|^2) / (|1 + \Gamma_S|^2 |1 + \Gamma_{opt}|^2) \quad 3.26$$

Also expressing

$$G_S = (1/Z_0) (1 - |\Gamma_S|^2) / (1 + |\Gamma_S|^2) \quad 3.27$$

Substituting these in equation 3.18, the obtained equation is:

$$F = F_{min} + (4R_N/Z_0) (|\Gamma_S - \Gamma_{opt}|^2 / [(1 - |\Gamma_S|^2) |1 + \Gamma_{opt}|^2]) \quad 3.28$$

For the fixed value of F , we show that this result defines a circle in the Γ_S plane.

We define the noise figure parameter N , as

$$N = [|\Gamma_S - \Gamma_{opt}|^2 / (1 - |\Gamma_S|^2)] = (F - F_{min}) |1 + \Gamma_{opt}|^2 / (4R_N/Z_0) \quad 3.29$$

Which is constant, for a given noise figure and the set of parameters, R_N, F_{min} .

Simplifying the above equation the result obtained is:

$$|\Gamma_S - (\Gamma_{opt} / N + 1)| = [N(N + 1 - |\Gamma_{opt}|^2)]^{1/2} \quad 3.30$$

this result defines circles of constant noise figure with

centre $C_F = \Gamma_{opt} / N + 1$ and

radius $R_F = \frac{[N(N + 1 - |\Gamma_{opt}|^2)]^{1/2}}{N + 1}$

4. Cryogenics

4.1 Effect of cooling on GaAsFET

The GaAsFET is the device used for low noise amplification at microwave frequencies. One can get minimum noise from these devices over a wide range of frequency. The noise figure achieved is quite good at room temperature since the thermal noise is the main noise source, a further reduction of noise can be achieved by cooling the device.

To understand the reasons behind cooling the device, consider the main noise sources that have already been mentioned, they are:

- 1) Intrinsic noise
- 2) Extrinsic noise

The intrinsic noises are the channel noise and the noise induced at the gate. They are highly correlated. The effect of the intrinsic noise can be minimized by optimally tuning the impedance of the source. By doing this the gate noise can be made to cancel with the channel noise.

But the extrinsic noise, which is mainly thermal in nature, is produced by the resistances like R_g , R_s , and R_d . This noise is highly temperature dependent and can be minimized by operating the transistor at a very low temperature.

The reduction in temperature is obtained by cooling the amplifier in a cryocooler system to liquid nitrogen temperature (77 K).

To justify that the low cooling enhances the performance of the amplifier consider the equivalent circuit of GaAsFET which is shown below,

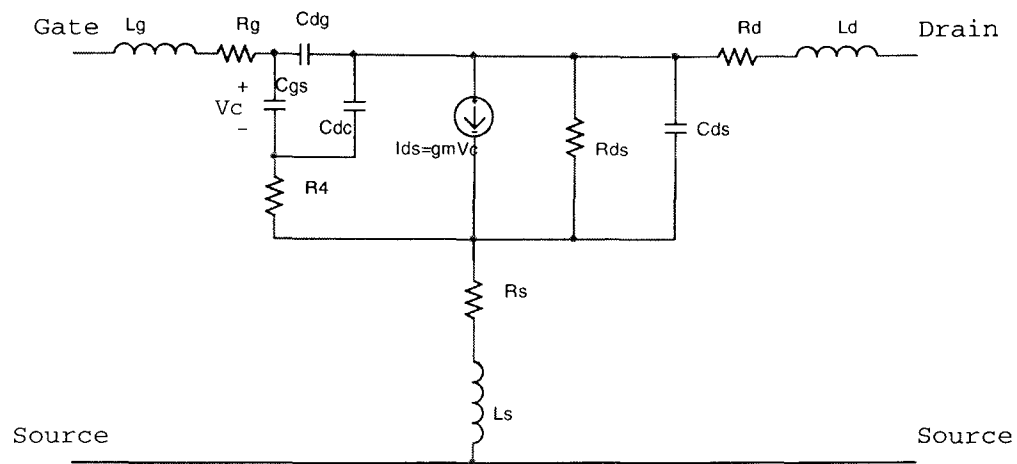


Fig.4.1 equivalent circuit of GaAsFET

Where;

Intrinsic elements

Cdg= drain to gate capacitance.

Cgs=gate to source capacitance.

Ri=input resistance.

ids= drain to source current.

Rds=drain to source resistance.

Extrinsic elements

Rd=drain resistance

Rg=gate resistance

Cds=drain to source capacitance.

Rs=source resistance

For low noise FET's, there are few relations mentioned which relates the minimum temperature and the various device parameters.

$$T_{\text{MIN}} = T_0 K_f (f/f_T) (g_m (r_g + r_s))^{-1/2} \quad 4.1$$

Where;

T_{MIN} = minimum noise temperature

T_0 = standard temperature 290 K

f_T = intrinsic cut-off frequency.

g_m = transconductance

r_g = gate parasitic resistance

r_s = source parasitic resistance.

From eqn.4.1 we obtain, transconductance is inversely proportional to the channel resistance. To achieve minimum noise it is desirable to have higher value of transconductance. Since at lower temperature the resistance of the semiconductor is low, the channel current increases which results in increase in the value of the transconductance. Therefore by cooling we can achieve lower noise.

Another approximate equation gives that:

$$T_{\text{MIN}} = 2(f/f_T)(r_t T_g g_{ds} T_d)^{-1/2} \quad 4.2$$

Where;

T_g =gate temperature.

T_d =drain temperature.

$r_t = r_s + r_g + r_{gs}$

r_{gs} =intrinsic gate resistance.

From the equation 4.1 and 4.2 we can analyze that,

Minimum temperature (T_{MIN}) is inversely proportional to transconductance (g_m)

Also, we have the relationship between intrinsic cut off frequency (f_T) and the g_m as

$$f_T = g_m / (2 * 3.14 * C_{gs}) \quad 4.3$$

f_T is directly proportional to g_m .

Hence, by decreasing the temperature intrinsic cut-off frequency can also be increased.

Putting in other words, from equations 4.1 and 4.2, we can infer that by increasing value of f_T and reducing the value of r_g and r_s , we can achieve low noise temperature.

As r_g and r_s are the parasites existing at the room temperature, cooling the device would definitely reduce the r_g and r_s and thus the noise figure.

There exists a limit up to which, when the amplifier is cooled, the noise figure gets reduced, but cooling below this limit does not cause the improvement in the noise figure as the device will have its minimum noise power that cannot be reduced.

The effect on the capacitance when cooled was experimentally was found to be:

- 1) Gate to source capacitance (C_{gs}) increases.
- 2) At the lower temperature, the drain to gate feedback capacitance (C_{gd}) is

smaller and the capacitance of the dipole layer in the channel (C_{dc}) are sufficiently larger. These changes are primarily due higher drain current, which results to large charge accumulation in the channel.

3) The negative space charge in turn causes the depletion layer to widen towards the drain, thus reducing the drain feedback capacitances.

From the above discussion it is now well justified that the cooling of the amplifier will enhance the performance of the low noise amplifier by not only reducing the noise temperature but also by providing improved gain because of the increase in the transconductance at lower temperature.

The following figures the variations of gain, noise figure, transconductance as a function of temperature.

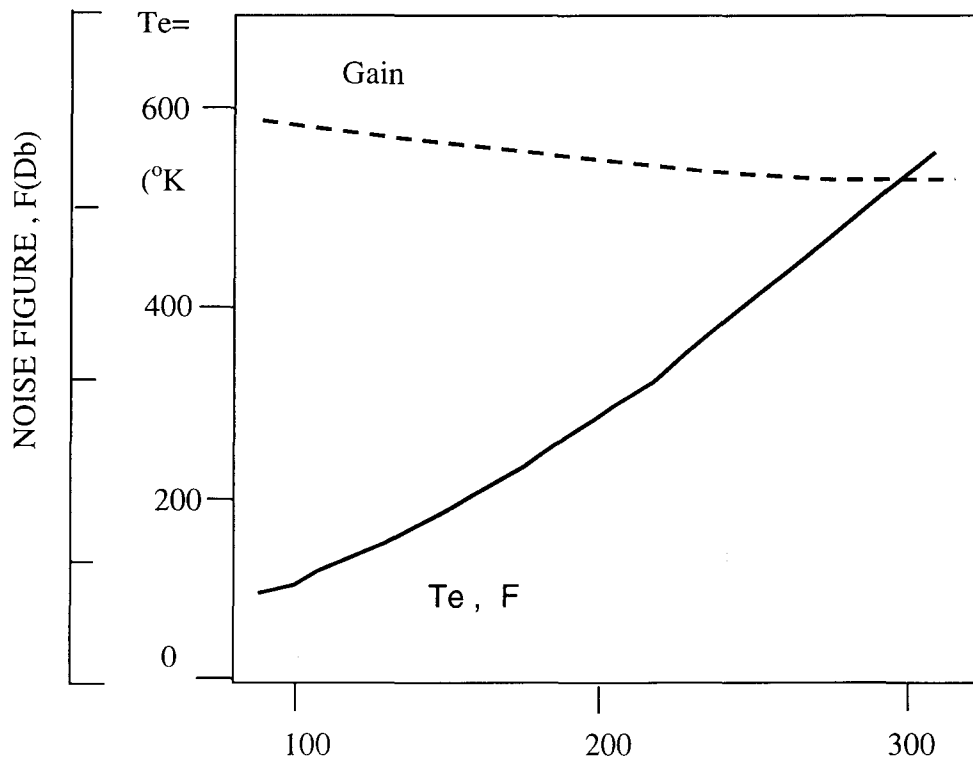


Fig 4.2 Minimum noise figure, equivalent input noise temperature, and the associated power of the GaAs MESFET versus ambient temperature

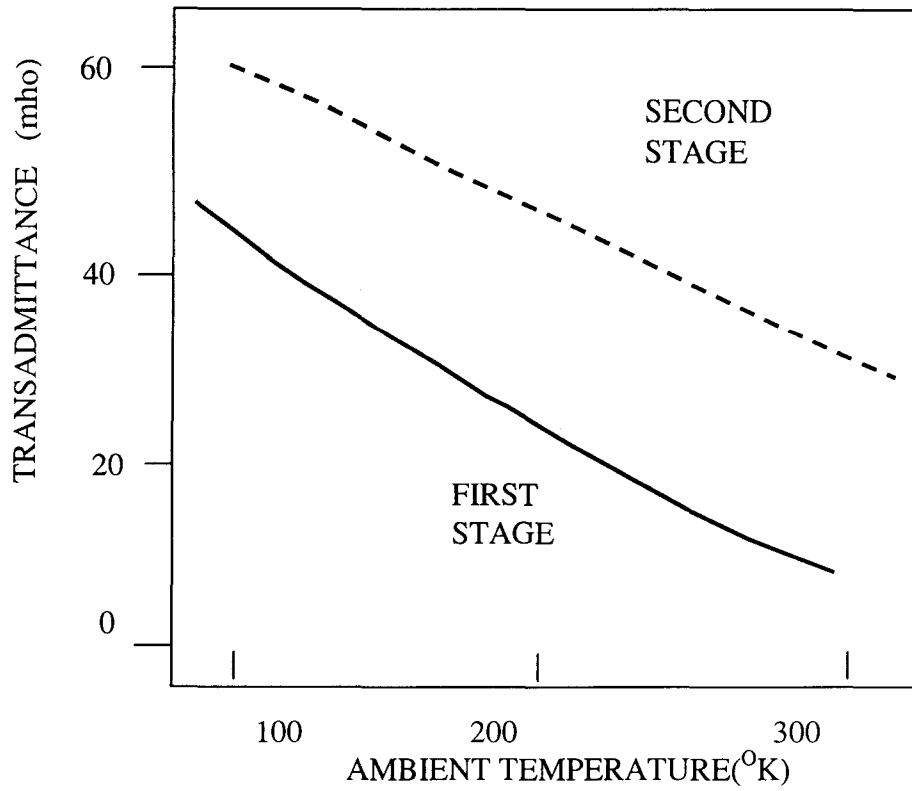


Fig 4.3 Transadmittance versus ambient temperature for the MESFET's operated in two stage

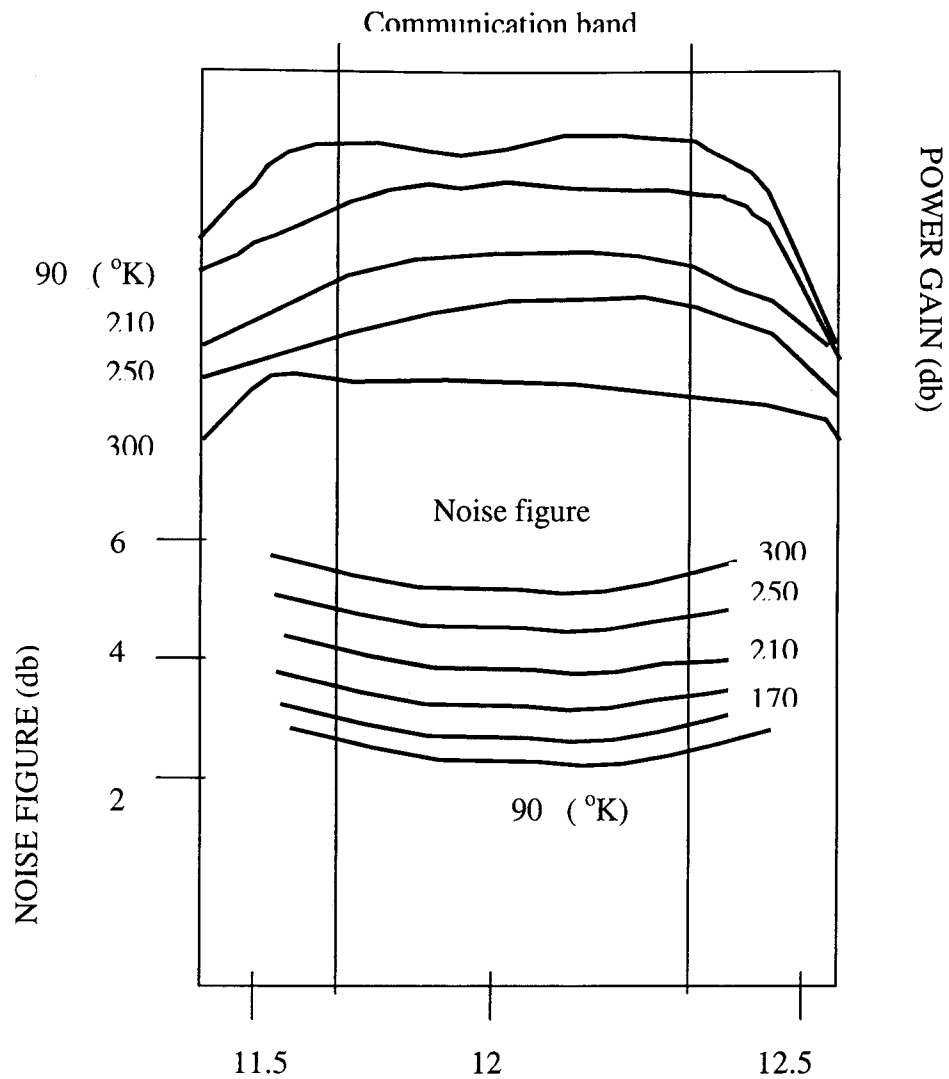


Fig 4.4 Variation of noise figure and gain with temperature

4.2 Design aspects of the Cooling System based on the Cryocooler:

The Low Noise Amplifier, which is to be cooled to cryogenic temperature, is made of copper. This will be mounted on the Cold head of a Cryocooler, through an intermediate base plate. A Stainless steel evacuated chamber is required to minimize the heat transfer from ambient to the cold surface. This Chamber will be henceforth *Vacuum Jacket*.

The Vacuum Jacket has various connectors for making electrical connections with the amplifier mounted inside. It also has a suitable coupling, which can be connected to a vacuum pump for evacuating the same. Thus, the basic units of a cryogenic cooling system are (a) Cold Head with the Low Noise Amplifier, (b) Vacuum Jacket and (c) Linear motor compressor of the Cryocooler and (d) Vacuum system for evacuation.

4.3 Design of the housing for the low noise amplifier

The low noise amplifier electronics is housed in a rectangular shaped box of size approximately 10cm x 5cm x 3cm made of copper. Stainless steel semirigid cables carry the RF signals from the amplifier. The Phosphor Bronze wires supply the bias required. This amplifier box will be rigidly fixed to the cold head of the Cryocooler. This assembly will be wrapped by several layers of super insulation to prevent radiation.

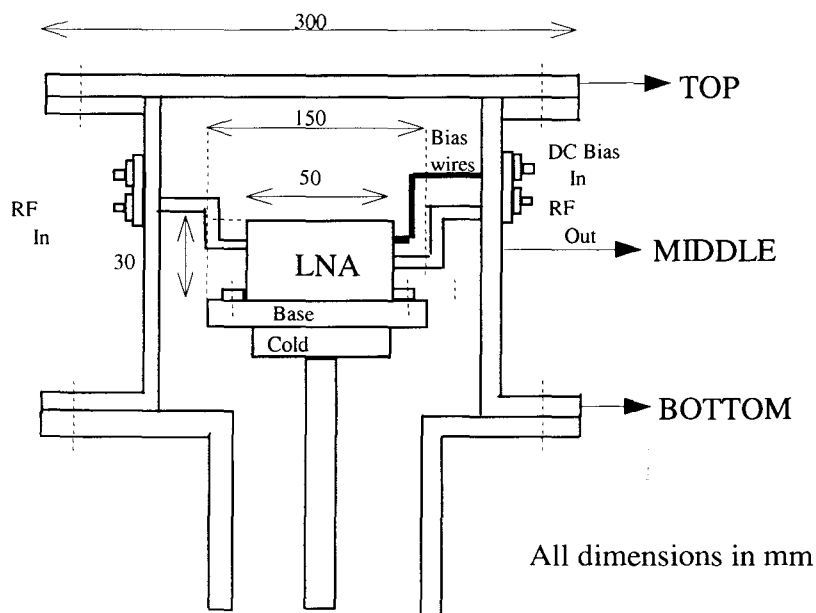


Fig. 4.5 Schematic of Low Noise Amplifier mounted on the cold head and surrounded by Vacuum Jacket.

4.4 Preliminary design of the Vacuum Jacket

The Vacuum Jacket is made of three separable parts – (i) Top flange (ii) Middle cylinder (iii) Bottom flange. This enables complete access to the components mounted on the cold head. This has suitable openings along with end couplings to enable evacuation of the Vacuum Jacket. This also has suitable openings for mounting vacuum feedthroughs and connectors for carrying dc bias and RF signal.

4.5 Estimation of Thermal Load to the Cold Head of the Cryocooler.

Heat transfer to the cold head occurs through the following mechanisms.

- Conduction and
- Radiation

It is assumed that the entire amplifier box, the intermediate base plate and the cold head are at an average temperature of 100 K after thermal stabilization. The vacuum jacket is maintained at ambient temperature of 300K.

4.5.1 Heat transfer due to conduction

The main contributors for the conduction heat transfer are

- Phosphor bronze Wires carrying DC bias to the amplifier
- Coaxial cable carrying RF signal to the amplifier
- Gas conduction.

4.5.1.1 Conduction heat transfer due to phosphor bronze wires

The phosphor bronze wires used for carrying the DC bias are thin and has a diameter equal to 0.5 mm. The length of the wire used is approximately 6 inches.

The heat transfer due to conduction is given by,

$$Q_1 = \frac{(k A \Delta T)}{L}$$

Where

k : Thermal Conductivity of the material

A : Area of cross section of the material

ΔT : Temperature gradient across the material

L : Length of the wire

For phosphor bronze wire we have

$$K = 66 \text{ mW/m K}$$

$$A = \pi r^2$$

$$= \pi(2.5 \times 2.5) 10^{-8} \text{ Sq. m}$$

$$\Delta T = (300 - 100) \text{ K}$$

$$L = 15.24(10^{-2}) \text{ m}$$

Substituting these values in the above equation we get the total conduction heat transfer, as $Q = 0.017006 \text{ W}$ for one Phosphor Bronze wire. Now, there are 5 wires carrying the signal in one unit, the heat conduction is given by $Q = 0.08503 \text{ W}$.

$$Q_1 = 0.08503 \text{ W} \quad 4.4$$

4.5.1.2 Conduction heat transfer due to co-axial cable

The co-axial cable used was made of stainless steel cable having an outer diameter of 3.6mm and inner center conductor diameter of 1mm. The total heat transfer due to this cable comes from both outer conductors as well as from inner conductor. It is assumed that one end of

the cable is held at 300 K and other end is at 100 K(ΔT) and thermal conductivity of the steel wire 'k' is 50.2 W/mK.

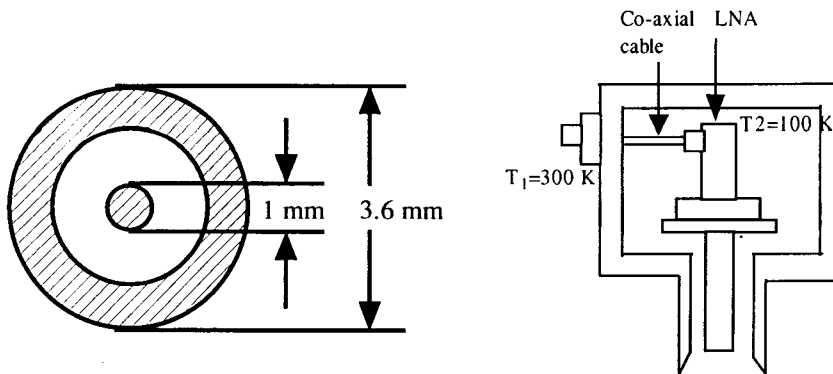


Fig .4.6 Cross section of the Stainless Steel coaxial cable and its arrangement inside Vacuum Jacket.

Total heat loss = Loss due to the outer conductor + Loss due to the inner conductor

The cross sectional area of the outer conductor is given by

$$A_1 = 2\pi(1.8)(10^{-3})(0.5)(10^{-3}) = (5.6548)(10^{-6}) \text{ m}^2$$

The cross sectional area of the inner conductor is given by

$$A_2 = \pi r^2 = \pi \times 0.5 \times 0.5 \times 10^{-6} = (0.7853) \times (10^{-6}) \text{ m}^2$$

The total cross sectional area is equal to $A = (6.4402) \times (10^{-6}) \text{ m}^2$

The length of the cable is 6 inches the total heat transfer due to one cable according the formula is given by

$$Q = \frac{(50.2)(6.4402)(10^{-6})(200)}{(15.24) \times (10^{-2})}$$

$$= 0.42427 \text{ W}$$

The heat transfer due to two cables (both input and output) is given by

$$Q_2 = 0.84855 \text{ W} \quad 4.5$$

Total heat transfer by conduction $Q_1 + Q_2 = 0.93358 \text{ W}$

4.5.1.3 Conduction heat transfer due to gas:

The heat transfer through the gas conduction was assumed to be negligible.

4.5.2 Heat transfer due to radiation

4.5.2.1 Radiation heat transfer between Vacuum Jacket wall and Cold head

The radiation heat transfer between two surfaces is given by

$$Q = \sigma A \varepsilon (T_1^4 - T_2^4)$$

Where

- σ - Stephen Boltzman constant = $5.67(10^{-8}) \text{ W-m}^{-2}\text{-K}^{-4}$
- A - Area of total cold surface at 100K – m^2
- T_1 - Temperature of the Vacuum Jacket = 300 K
- T_2 - Temperature of the Cold Head = 100 K
- ε - Emissivity of Stainless steel = 0.06

The area of the cold surface is the total exposed area of the various components such as the Low Noise Amplifier box, supporting copper base plate and the cold head of the Cryocooler. Using the dimensional data of the above components, this area was calculated to be 0.0450m^2 .

Substituting these values in the above equation, the radiation heat transfer is given by

$$\begin{aligned} Q &= 5.67(10^{-8}) \times (8.1 \times 10^9 - 0.1 \times 10^9) \times (0.06) \times (0.0450) \\ &= 5.67 \times 10^{-8} \times 8 \times 10^9 \times 0.06 \times 0.0450 \\ &= 1.2247 \text{ W} \end{aligned}$$

We assumed that about 10 layers of super insulation is wrapped around the entire cold surface. In this case, the radiation heat transfer reduced approximately by a factor of 11.

Hence, the radiation heat transfer due to the above was calculated as

$$Q_3 = 0.1113 \text{ Watts} \quad 4.6$$

4.5.2.2 Radiation heat transfer to the Coaxial cable from the Vacuum Jacket

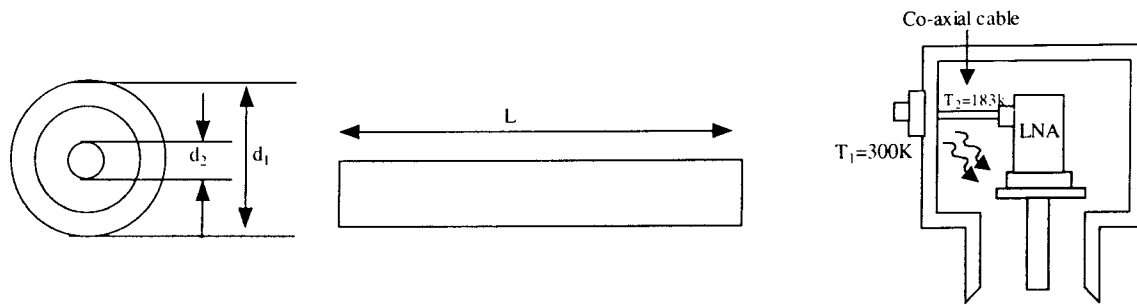


Fig.4.7 Schematic diagram of stainless steel coaxial cable and its arrangement inside Vacuum Jacket

The radiation heat transfer in a coaxial cable will occur on the outer conductor of the cable. If d_2 is the diameter of the outer conductor (= 3.6 mm), then the area of exposure is given by

$$A = \pi d_2 h = \pi 3.6 \times 10^{-3} \times 15.4 \times 10^{-2} = 1.7236 \times 10^{-3} \text{ sq. m.}$$

Hence

$$Q = 5.67 \times 10^{-8} (0.06) \times 1.7236 \times 10^{-3} [300^4 - 183^4]$$

$$= 0.04091 \text{ Watts}$$

and for two cables, $Q = 0.08182 \text{ Watts.}$

Here the mean temperature of the cable is calculated as the log mean temperature between the ends of the cable. This value is equal to 183 K.

As before if one insulates the coaxial cable with with 10 layers of superinsulation, this heat transfer gets reduced by a factor of 11. If the heat transfer is calculated for two cables, the total heat transfer is given by

$$Q = 0.00744 \text{ Watts}$$

Total heat transfer by radiation from the Vacuum Jacket wall to the RF cables is given by

$$Q_4 = 0.00744 \text{ W} \quad 4.7$$

4.5.2.3 Radiation heat transfer to the DC bias wires from the Vacuum Jacket

As mentioned earlier the DC bias wire has a diameter of 0.5 mm. The area of exposure is given by

$$\text{Area} = 2\pi rh$$

$$= \pi dh$$

$$= \pi (0.5) \times (10^{-3}) \times (15.24) \times (10^{-2})$$

$$= (2.393) \times (10^{-4}) \text{ Sq. m}$$

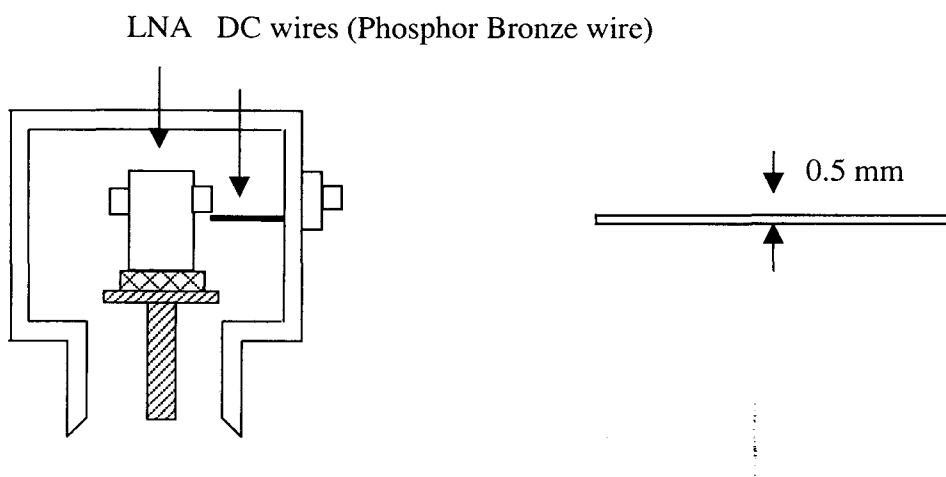


Fig.4.8 Cross Sectional view of the Phosphor Bronze wire and its arrangement inside Vacuum Jacket

Therefore the radiation transfer due to the cable is given by

$$\begin{aligned} Q_5 &= \sigma A \varepsilon (T_1^4 - T_2^4) \\ &= (5.67)(10^{-8})(2.393)(10^{-4})(0.06)(300^4 - 183^4) \\ &= 5.681 (10^{-3}) \\ &= 0.005681 \text{ Watts} \end{aligned}$$

For 5 numbers of DC wires, the total heat transfer is equal to 28.40 mW. This can be reduced further by surrounding them with superinsulation layers.

TOTAL HEAT FLUX CALCULATION

1. CONDUCTION (W)

$$Q_{(1)} = 0.08503$$

$$Q_{(2)} = 0.84855$$

$$\text{Total} = 0.93358 \text{ Watts}$$

2. RADIATION (W)

$$Q_{(3)} = 0.1113$$

$$Q_{(4)} = 0.00744$$

$$Q_{(5)} = 0.02840$$

$$\text{Total} = 0.14714 \text{ W}$$

Result:

The total estimated heat transfer due to both conduction and radiation is $\cong 1.0807$ Watts, for the above configuration.

The above heat transfer was recalculated assuming that one uses 1 mm diameter DC bias wires in place of 0.5 mm wires. In this case, the heat transfer is calculated to be ~ 1.3642 Watts.

5. AMPLIFIER DESIGN

The design of the two stage HEMT amplifier has been presented here. The amplifier is designed for the following specifications:

Frequency range of operation	=	0.5GHz-1.5GHz
Center frequency	=	1000MHz
Bandwidth	=	1000MHz
Gain	=	20dB
Pass Band Ripple	=	0.5dB
Noise figure	=	as low as possible
Input return loss	=	Less than -10dB

The design and performance analysis of the amplifier make use of the GENESYS RF CAD package.

5.1 General Amplifier Block Diagram

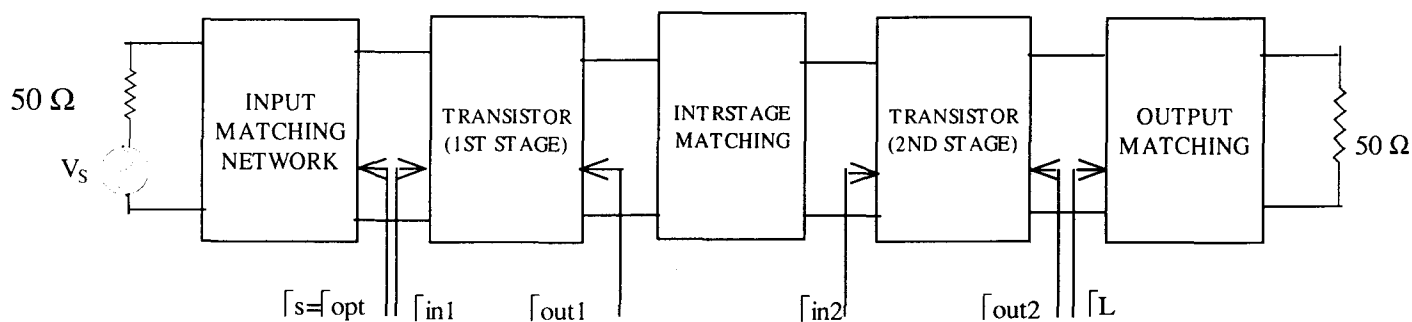


Fig 5.1 General block diagram of the two-stage amplifier

The above figure shows the general block diagram of the two-stage amplifier. The parameters used are explained below:

Γ_s represents the first stage source reflection coefficient.

Γ_{opt} represents the optimum reflection coefficient

Γ_{in1} represents the Input reflection of first stage.

Γ_{out1} represents the output reflection coefficient of first stage.

Γ_{in2} represents the Input reflection coefficient of second stage.

Γ_{out2} represents the Output reflection coefficient of second stage.

Γ_L represents the load reflection coefficient.

The amplifier has an input matching network, inter-stage matching network and an output-matching network. The input-matching network transforms source impedance to the optimum impedance of the first stage transistor for minimum Noise figure. The inter-stage matching section matches the output impedance of the first stage transistor to the input impedance of the second stage transistor for maximum gain. The output-matching network transforms output impedance of the second stage transistor to the load impedance.

5.2 Selection of Transistor

The selection of the transistor is made based on the frequency of operation, noise figure and optimized reflection co-efficient.

We have chosen the High Electron Mobility Transistor – Fhx35lg to build the amplifier in the frequency range mentioned earlier since it has got lowest Noise figure over the entire range.

The parameters at 1GHz are obtained by extrapolating the values given in data sheets. The parameter values are listed below (at 1GHz):

Device: FUJITSU Fhx35lg HEMT

Parameter	Magnitude	Angle (degrees)
S11	23.52	-87.6
S21	158.56	88.38
S12	73.1	89.98
S22	19.9	-88.52

Bias conditions:

$V_{ds}=3v, I_{ds}=10 \text{ mA}$

Noise parameters:

Table 5.1

Frequency (GHz) (dB)	NF_{min}	Γ_{OPT}		$R_n/50$
		MAG	ANG	
0.5	0.323	0.912	5.762	0.7
0.6	0.329	0.904	7.544	0.692
0.7	0.334	0.896	9.324	0.684
0.8	0.339	0.888	11.10	0.676
0.9	0.344	0.881	12.87	0.608
1	0.349	0.873	14.64	0.660
1.1	0.354	0.866	16.41	0.652
1.2	0.359	0.859	18.17	0.644
1.3	0.364	0.852	19.92	0.636
1.4	0.370	0.846	21.67	0.628
1.5	0.375	0.839	23.42	0.620

5.3 Stabilizing the transistor using feedback

5.3.1 Stability Factor

The stability factor K was calculated from 0.5 to 1.5GHz and found to be less than 1 as shown in table 5.2. This implies that the transistor is potentially unstable at these frequencies and has a tendency to oscillate. The input and output impedances for which the amplifier oscillates lie in a region between the Smith chart and the overlapped stability circle. This is shown in Fig 5.3. The constant gain circles, constant noise circles (Fig.5.4) and stability circles (Fig.5.4 and Fig.5.5) were drawn using the GENESYS RF CAD package. It was found that the centers of the circles that represent maximum gain

and minimum noise figure respectively were far separated. This means it is not possible to simultaneously match gain and noise for this transistor at this frequency.

Table5.2

Frequency	K Factor
500	0.102
562	0.11
625	0.117
687	0.122
750	0.126
812	0.129
875	0.132
937	0.134
1000	0.135
1062	0.143
1125	0.149
1187	0.156
1250	0.161
1312	0.167
1375	0.172
1437	0.177
1500	0.181

To overcome both the problems of stability and simultaneous matching of noise and gain, a small inductance is added from source to ground, which acts as a loss less series feedback. Since the value of k was found to be less than 1, the value of the inductor in the feedback is varied till the value of k becomes greater than 1. The modified value of source inductance that makes k factor greater than 1, at the frequency range specified, was found to be 5.83nH. The stability circles and the k factor after addition of the feedback is as shown in fig 4.5 in table 4.3 respectively.

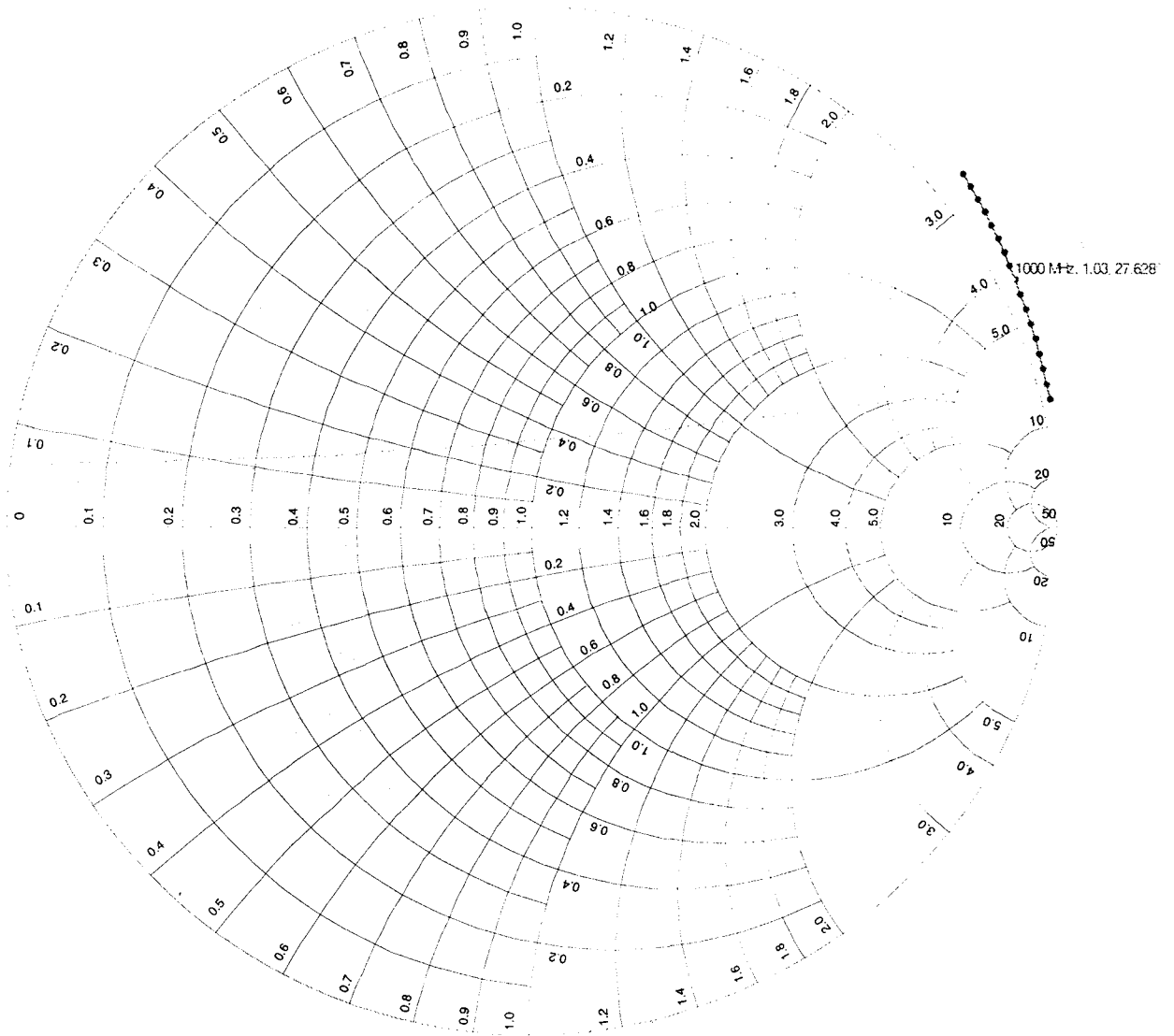


Fig 5.2 Input and output stability circles before putting the feedback inductor

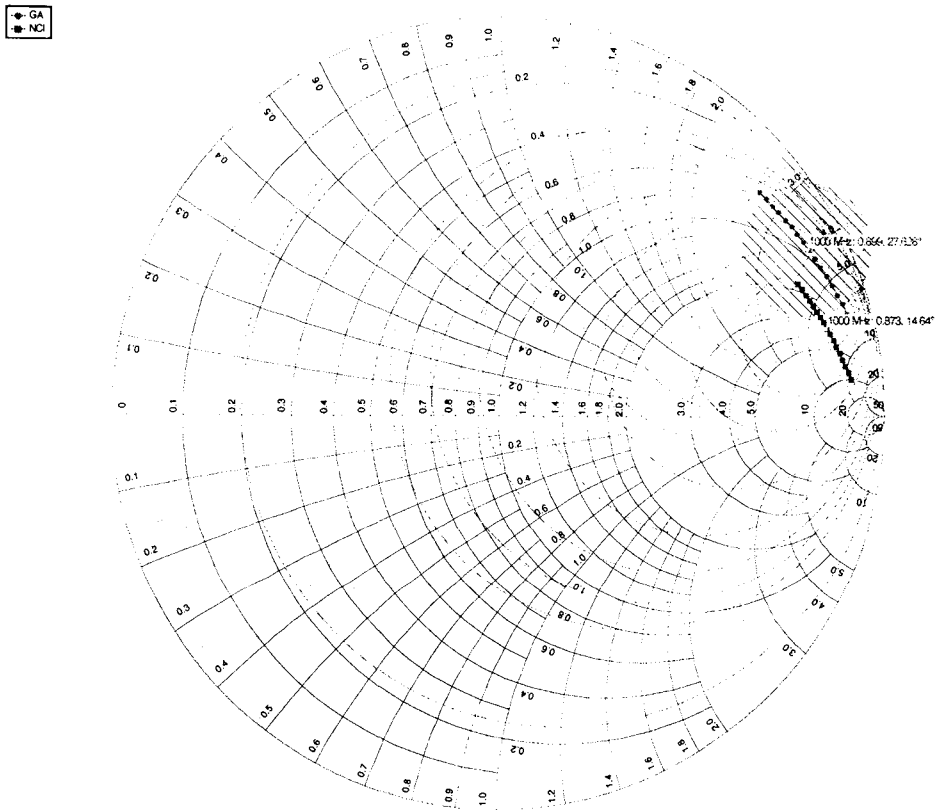


Fig 5.3 Gain and noise figure circles

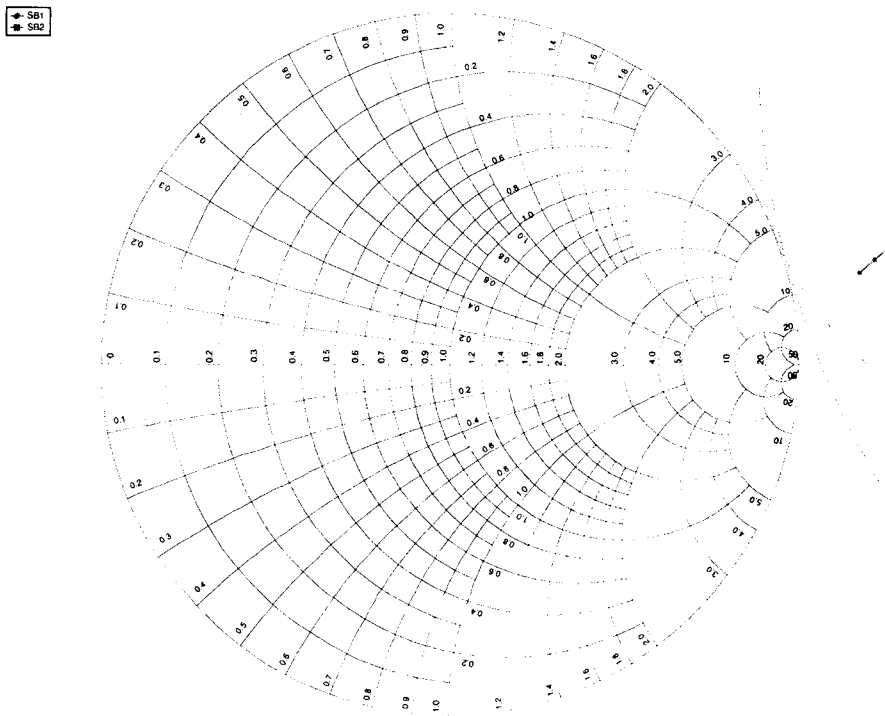


Fig 5.4 Input and output stability circles after putting feedback inductor

Table 5.3

Frequency	k factor
500	1.000
562	1.002
625	1.009
687	1.013
750	1.015
812	1.016
875	1.015
937	1.013
1000	1.011
1062	1.011
1125	1.009
1187	1.008
1250	1.006
1312	1.003
1375	1.002
1437	1.001

5.3.2 Lossless Feedback

Equation 3.18 shows that when $\Gamma_s = \Gamma_{opt}$, the noise figure of the network becomes minimum. However, by doing so, we may have to sacrifice some gain, since, one of the condition for gain to be maximum is

$$\Gamma_s = \Gamma_{in}^*$$

Therefore it is not possible to have maximum gain with minimum noise.

Hence, one of the basic problems is the significant difference between the desired source impedances for optimum noise and input match. In such a case, some form of isolator is needed at the input to maintain a reasonable input match when the device is operating at its minimum noise figure.

Lossless feed back elements can transform, the input and optimum noise source impedances until simultaneous or acceptable compromise is reached. However the reactive

feedback will change the minimum noise figure as well as optimum noise source impedance. In addition, the gain and the stability factor of the circuit will also change.

For series feed back, the noise figure will be raised by a small value of inductance and the gain correspondingly gets reduced. Minimum noise measure (M_{\min}) remains invariant to lossless feedback effects, where M_{\min} is given by

$$M_{\min} = f_{\min}/(1-1/g_{av})$$

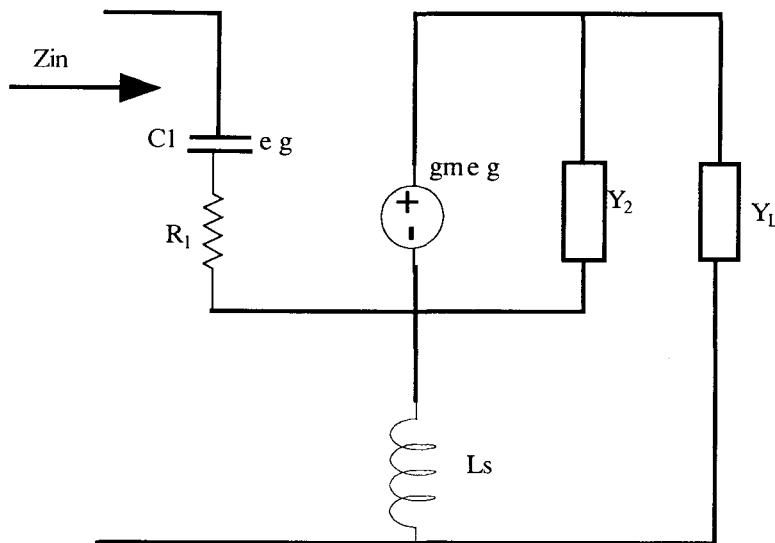


Fig 5.5 Equivalent circuit of a FET with source inductance

Fig. 5.5 shows the simplified equivalent circuit of a FET with source inductive feedback. If we assume that the impedance due to L_s is very small compared to $1/Y_2$ and $1/Y_L$, the expression for Z_{in} can be written as,

$$Z_{in} = R_1 + (1/j\omega C_1) + j\omega L_s + g_m L_s / [C_1 + (1 + Y_2/Y_L)] + (\omega L_s)^2 Y_2 / [1 + Y_2/Y_L]$$

If $Y_L \gg Y_2$ and $\omega C_1 \ll g_m$, expression for R_{in} reduces to

$$R_{in} = R_1 + g_m L_s / C_1$$

As can be seen from the above equations, addition of a small value of L_s , causes the real part of Z_{in} to change drastically, while the imaginary part is almost the same. If R_{in} is increased to the value R_{opt} then we will obtain both the noise and power match.

For small value of L_s , the value of Z_{opt} changes by,

$$Z_{opt}' = Z_{opt} - j\omega L_s \text{ when } |\omega L_s| \ll |Z_{opt}|$$

So, the optimum reflection coefficient doesn't change much with the addition of L_s . But it can cause a small decrease in the gain. The common source S-parameters is converted to Z-parameters first. The Z-parameters of the series inductance L_s is also found out. They are then added together and inverse transformation is carried out. This yields the modified S-parameters of the device with source inductance feedback.

5.4 Design of matching sections:

One of the most important aspects of high frequency, circuit design is Impedance Matching. The basic idea of impedance matching is illustrated in the Fig 5.6. Impedance matching is required to obtain maximum power transfer between source and load. One of the most fundamental criteria is that a matching network must be ideally loss less to avoid unnecessary loss of power.

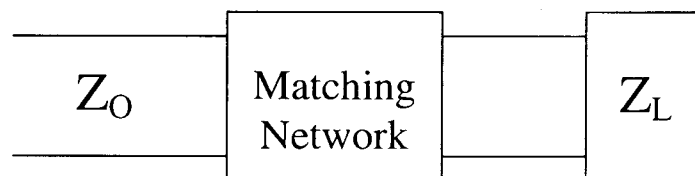


Fig 5.6 Loss less Network, matching arbitrary load impedance to a transmission line.

Impedance matching is necessary for various applications as mentioned below.

- Maximum power transfer between source and load.
- Minimum power loss in the feed line.
- Improvement in the signal to noise ratio of the receiver system by impedance matching sensitive receiver components like Antenna, Low noise amplifier, etc.
- Minimum noise contribution from the amplifier.
- Must operate over a wide range of frequency.

Different techniques of impedance matching networks are

1. Matching with lumped elements (L-Section)
2. Single stub tuning.
3. Double stub tuning.
4. Quarter wave transformer.
5. Multi-section transformer.
 - ❖ Binomial multi-section transformer.
 - ❖ Chebyshev multi-section transformer.
6. Tapered lines.
 - ❖ Exponential taper.
 - ❖ Triangular taper.
 - ❖ Klopfenstein taper.

We have utilized the matching technique using lumped elements and quarter wave transformer.

The Quarter-Wave Transformer

The transmission line input impedance equation is given by,

$$Z_{in} = Z_0 \times \frac{(Z_L + j Z_0 \tan (\beta l))}{(Z_0 + j Z_L \tan (\beta l))}$$

When the length of the transmission line is chosen equal to $\lambda / 4$, the above equation reduces to

$$Z_{in} = Z_0 \times \frac{(Z_L + j Z_0 \tan(90^\circ))}{(Z_0 + j Z_L \tan(90^\circ))}$$

$$Z_0^2 = Z_{in} \times Z_L$$

The quarter-wave transformer is simple and useful circuit for matching real load impedance to a transmission line. The additional feature of quarter wave transformer is that it can be extended to multiple sections in a methodical manner, for broader bandwidth. If only narrow band impedance match is required, a single section transformer may suffice. Single section quarter matching transformer circuit is shown in the figure 4.4. Characteristic impedance $Z_1 = \sqrt{(Z_0 \times Z_L)}$ section is,

The electrical length of the impedance matching section at the center frequency f_0 , is $\lambda_0 / 4$, but at other frequencies the length is different, so a perfect match ceases to exist.

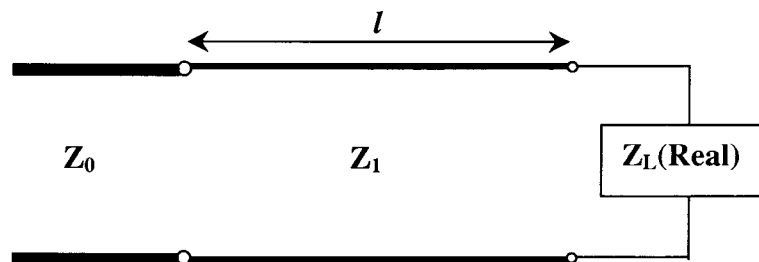


Fig 5.7 Single Section Quarter-wave Transformer of length l at center frequency f_0

5.4.1 Design of input matching section

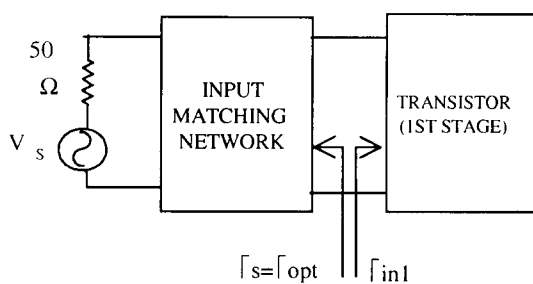


Fig 5.8

Input matching is done for the minimum noise of the transistor. Quarter-wave transformer sections and the lumped elements have been used to transform the source impedance to Γ_{OPT} of the HEMT at 1 GHz. The value of Γ_{OPT} was read at 1 GHz and was found to be .873(mag) ,14.647(ang). The corresponding impedance value is $164.5 + j303.5$. Hence 50Ω source was matched to 164.5Ω using quarter-wave transformer and an inductor of was used to cancel the capacitance part of the load.

5.4.2 Design inter stage matching section

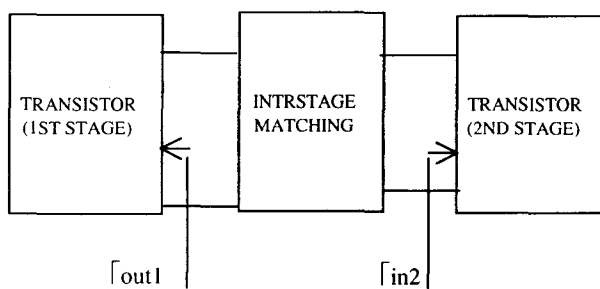


Fig 5.9

The interstage matching is done to deliver the maximum power from the first stage to the second stage .In this matching the output impedance of the first stage is matched to the input impedance of the second stage transistor.

The parameters for the interstage matching are:

$$S_{11} = 0.617 - j0.24 \quad Z_{out1} = 137 - j117$$

$$S_{22} = 0.861 - j0.118 \quad Z_{in2} = 368 - j354$$

The real part of Z_{out1} (137Ω) is converted to real part of Z_{in2} (368) with quaterwave transformer and the imaginary part is matched with an inductor of suitable value.

5.4.3 Design of output matching section

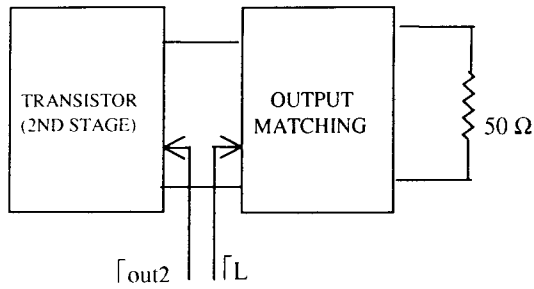


Fig 5.10

The value of S_{22} was read at 1GHz and the value of impedance corresponding to S_{22} was found to be $400.52 + 64.65j$. Hence 50Ω load was matched to 400.52Ω using quarter-wave transformer and an inductor was connected to account for conjugate of the imaginary part.

The width of the rectangular microstrip was calculated using Genesys for ULTRARAM PCB with ϵ_r value of 2.5 at the lower cutoff frequency 0.5 GHz.

The schematic of the overall amplifier circuit including the coupling capacitors, matching inductors and the transistor as realized using Genesys, is as shown in Fig.5.15.

The designed two stage amplifier can be represented as:

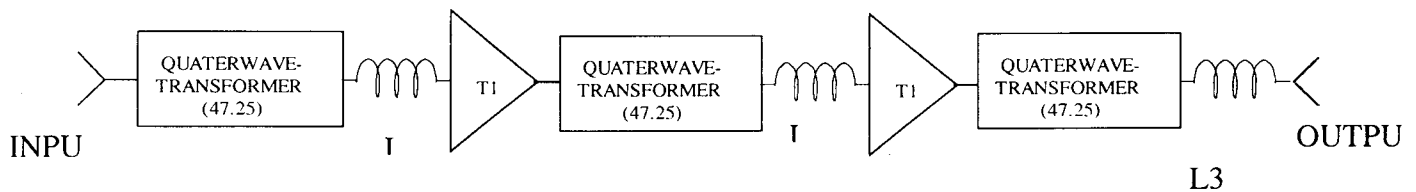


Fig 5.11

Where ;

$$L1 = 48.303 \text{ nH}$$

$$L2 = 37.79 \text{ nH}$$

$$L3 = 10.11 \text{ nH}$$

5.4.4 Modified design values after optimization:

The designed circuit was optimized with the help of CAD tool GENESYS over the frequency range of 0.5 Ghz to 1.5 Ghz .The modified design values for each stage is given below:

Modified input section



Fig 5.12

Inductor(L1) = 28.065 nH

Quarterwave transformer = 50 mm

Modified interstage section



Fig 5.13

Inductor(L2) = 20 nH

Quarterwave transformer = 16 mm

Modified output section



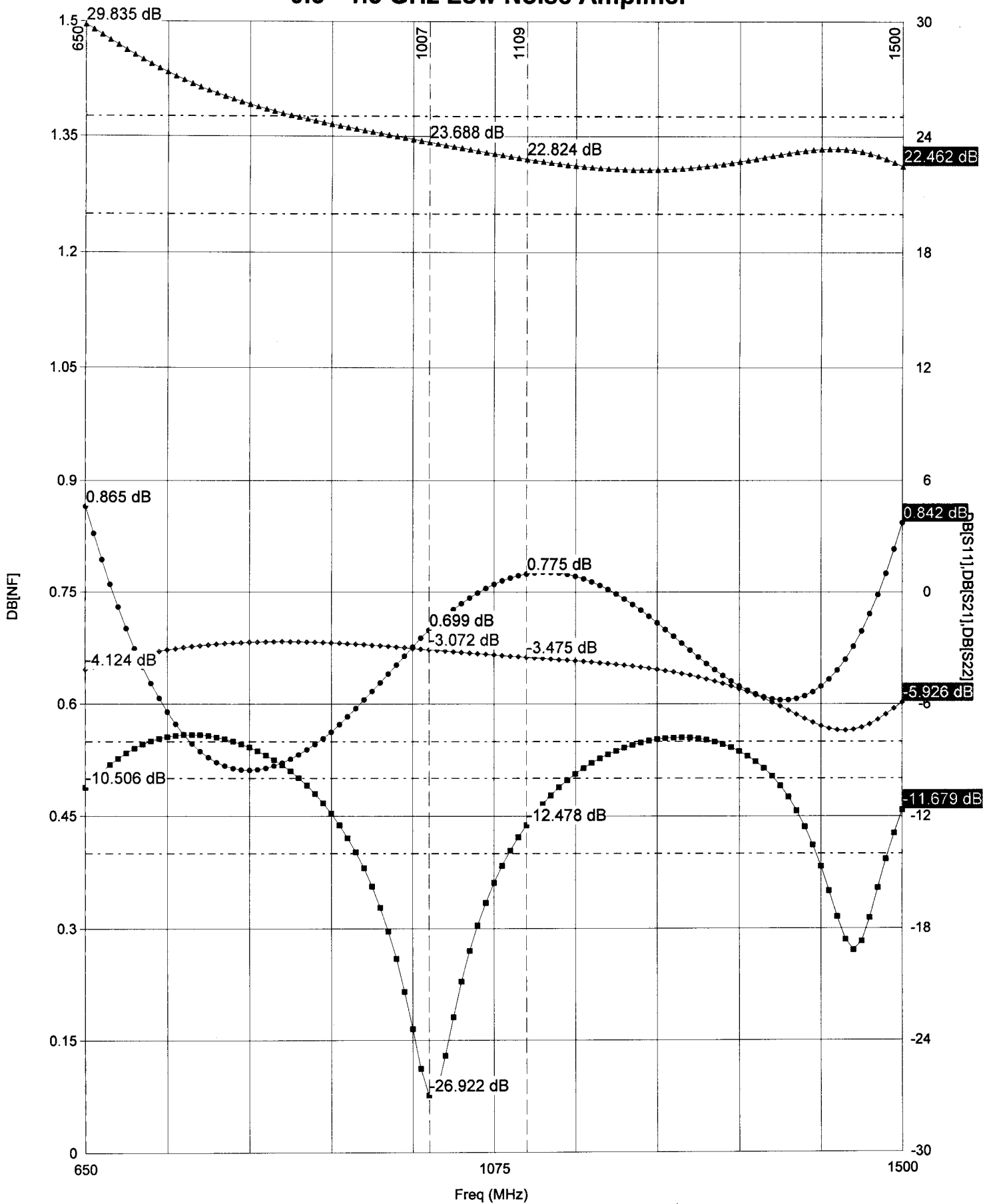
Fig 5.14

Inductor(L3) = 14 nH

Quarterwave transformer = 16mm

The schematic of the overall amplifier including the coupling capacitors , inductors, transistor and the bias circuit as realized using GENESYS is as shown in Fig 5.15 and the complete layout is shown in the Fig 5.16. The simulated response using CAD tool (GENESYS) is shown in Fig 5.17 .

0.5 - 1.5 GHz Low Noise Amplifier



● DB[NF] ■ DB[S11] ▲ DB[S21] ◆ DB[S22]

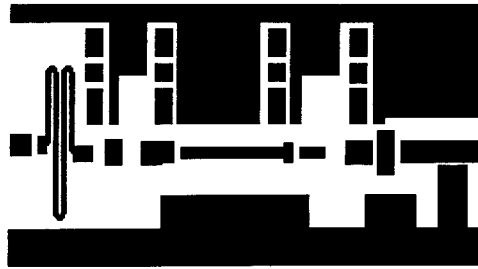


Fig 5.16 Layout of the low noise amplifier

5.5 Design of biasing section:

The DC bias voltage must be applied to the gate and the drain, without disturbing the RF circuit paths. This is done by using RF chokes with capacitors and the inductors.

The RF chokes provide very low DC resistance for the biasing, and a very high impedance at the RF frequencies to prevent microwave signals from being shorted by the bias supply. Similarly, the input and output decoupling capacitors block the DC.

The circuit used to provide biasing to the transistor is as shown in Fig 5.17. The resistance in the bias path is chosen such that the drain is maintained at 2V and a current of 10mA is passed through the device when 3V is applied to the bias. The bypass capacitors are chosen such that they offer very low impedance at the frequency of operation.

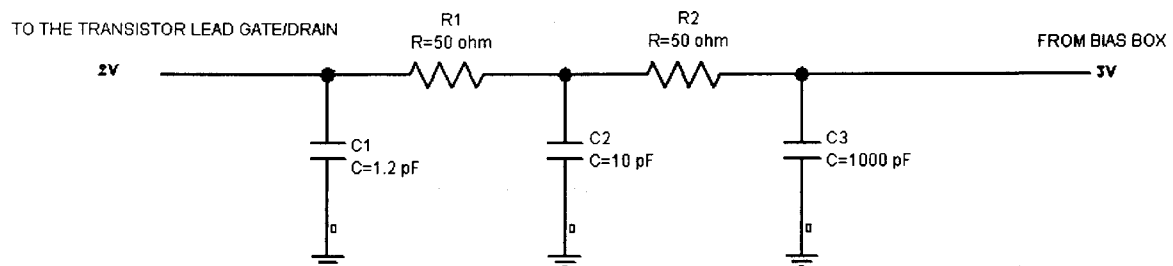


Fig 5.18 Biasing circuit for the transistor

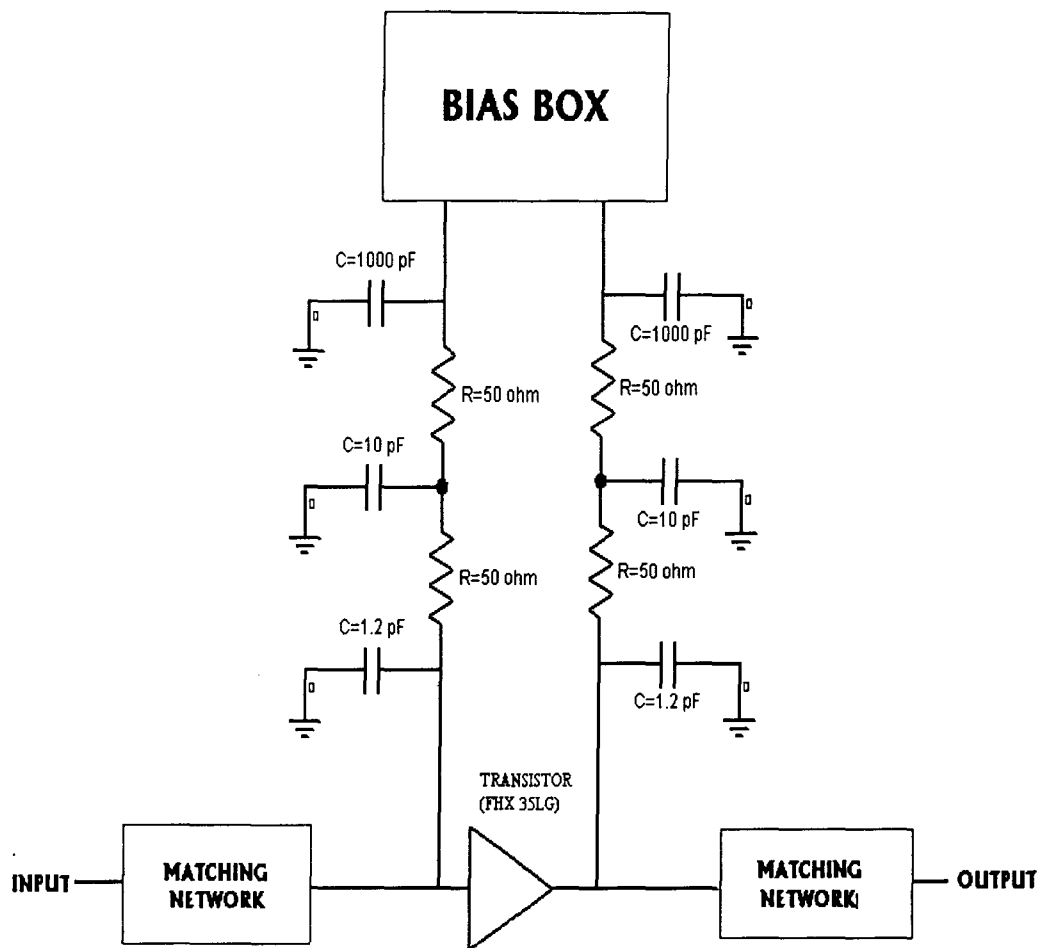


Fig 5.19

6. BUILDING AND CHARACTERIZATION OF THE LOW NOISE AMPLIFIER

6.1 Construction details of the amplifier

6.1.1 Development of the printed circuit board

The circuit was realized on ULTRARAM 2000 PCB from Rogers Corporation. ULTRARAM 20000 laminate is made of woven glass Teflon reinforced PTFE. This is designed for high reliability stripline and microstrip circuit applications. The dielectric constant ϵ_r of this laminate is typically 2.5. It has a low dissipation factor, $\tan\delta$ of 0.0022 maximum of 10 GHz.

6.1.2 Amplifier chassis

Amplifier is housed in a milled copper block. All the capacitors in the bias section were soldered directly on to the chassis. Enamelled copper wires (Gauge #27) were used for providing bias to the transistor. Bias was given to the amplifier from a separate bias box outside the amplifier (refer appendix for the circuit diagram and operation of the bias box).

SMA microstrip launchers from omni spectra Inc were used for input and output RF connections to minimize coaxial microstrip transition loss. Chip capacitors from American Technical ceramics Inc were used for both bypass and coupling capacitors -ATC 100B for 1000pF bypass capacitor and ATC 100A for the rest. The transistors were mounted on the holders and the drain and source leads were mounted in plane with the PCB to reduce any additional inductance added to the circuit due to the leads. The PCB was fixed to the chassis using screws. The mechanical diagram of the chassis is shown in Fig.6.1. The photograph of the amplifier is shown in Fig .6.2

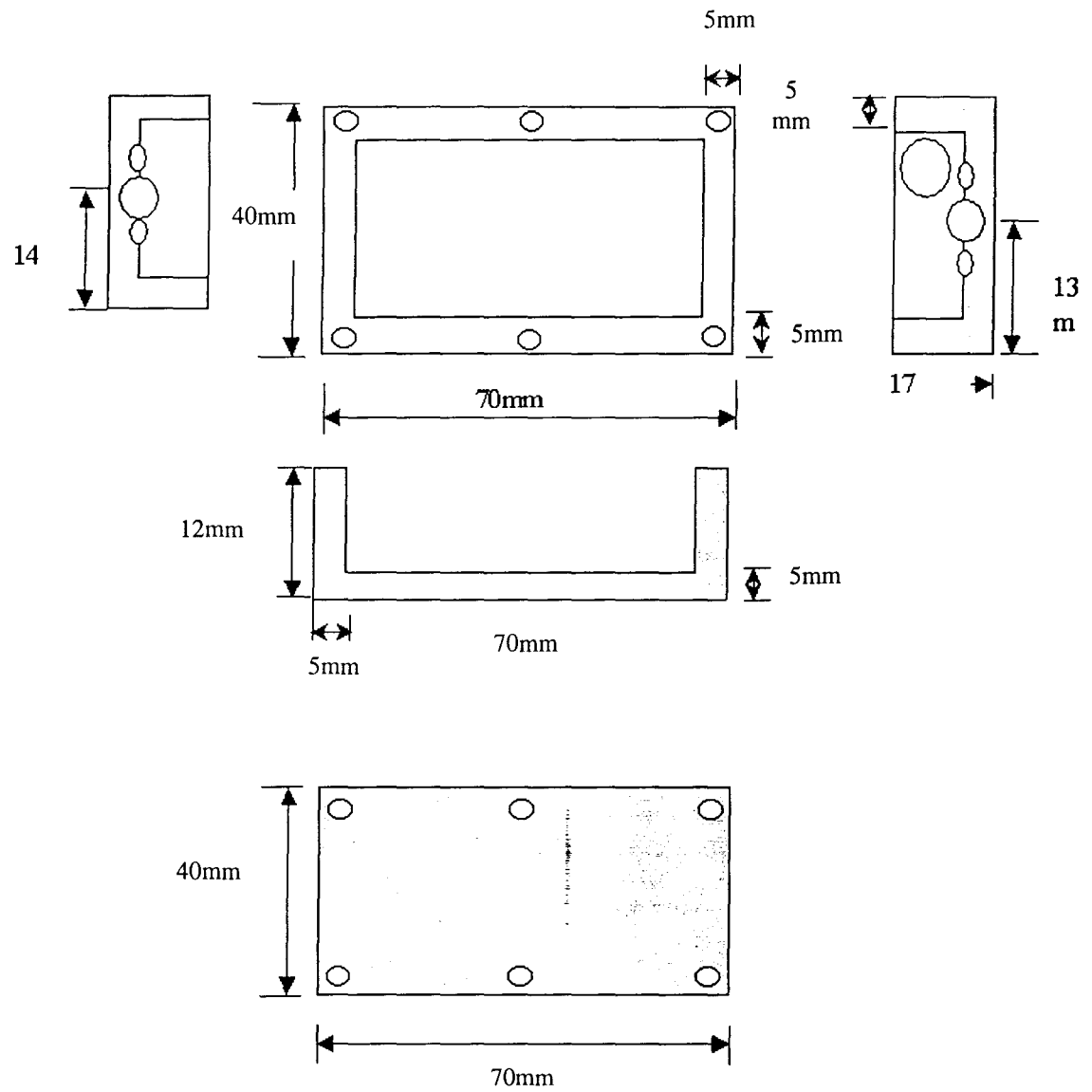
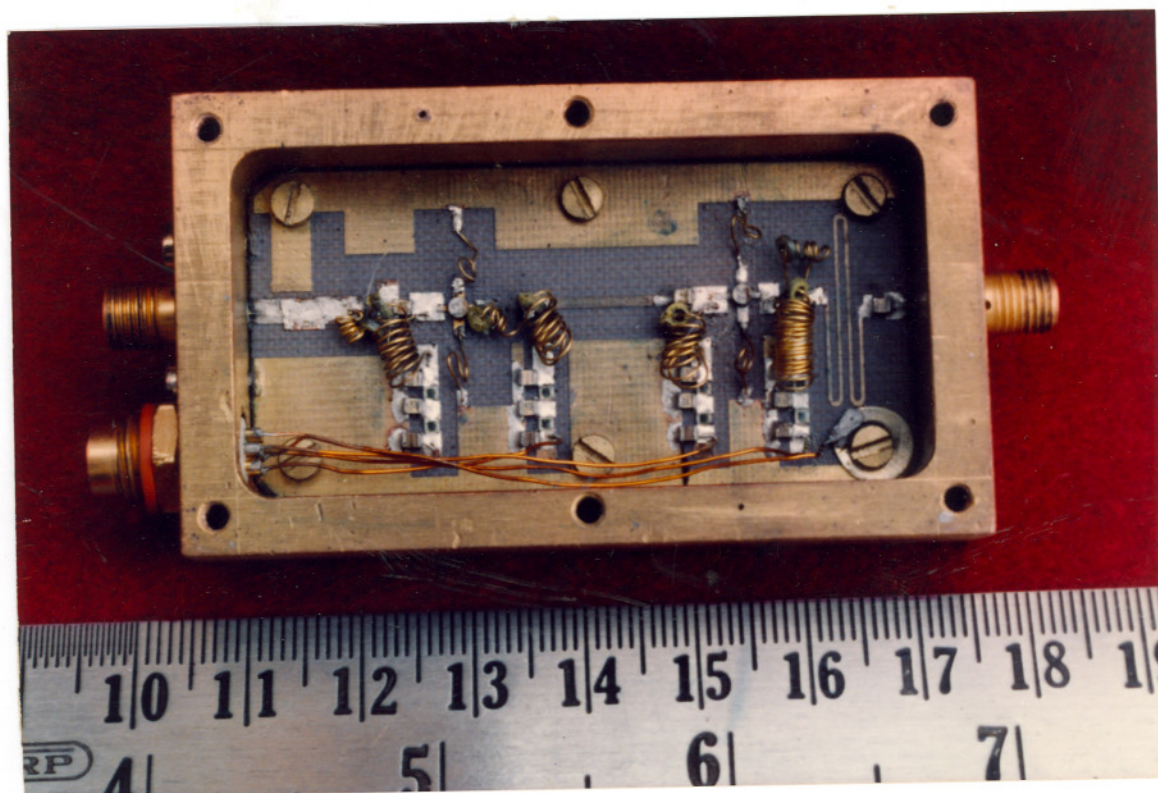


Fig 6.1



6.1.3 Amplifier assembling

LNA assembling is done as follows

1.Card sizing:

- a. The card is sized to exact dimensions.
- b. The sharp edges of the first transmission matching line, input 50Ω line and 50Ω output line were chamfered.

2.Card placing:

Using 10 BA screws of the right length the card was screwed down.

3.Placement Of Bypass Capacitors:

The procedure followed for the placement of bypass capacitors is as follows.

- a. Capacitors were placed in their respective positions .

- b. Capacitors were individually cleaned using toothpick, cotton and Isopropyl Alcohol (IPA).
- c. Chassis was immersed in Alcohol bath .
- d. Chassis was removed and allowed to dry.

4. Placement of resistors between by-pass capacitors:

- a. Two 50Ω resistors are soldered between 620 pf and 10 pf capacitors.
- b. Resistors between 10 pf and 1.2 pf were soldered only on top of 10 pf and the other side was soldered later while soldering the bias wires.
- c. Extra flux was cleaned using IPA, cotton and toothpick.

5. Bias for the amplifier:

- a. Gauge No.27 Enameled Copper wires cut to right length plus 1 cm were used between the bias connector and top of 620 pf by-pass capacitors.
- b. The wires were routed properly between the 620-pf capacitors and the chassis wall.
- c. For ground connection, a ground tag was used on end of the Copper wire and screwed onto the chassis.
- d. Extra flux was cleaned using IPA, cotton and toothpick.

6. Bias checking:

- a. Bias cable was connected to the connector.
- b. We set V_{d1} (drain voltage knob)=3V in the bias box and adjusted the I_d (drain current knob) to approximately 10 mA.
- c. The bias box was put on and checked for the bias on top of the 1.2 pf capacitor. ($V_g=2V, V_d=0.6V$)

7. Soldering of the transistor:

- a. The working table was cleaned thoroughly.
- b. The iron plate surface was cleaned thoroughly with sand paper.
- c. The grounding of Aluminium plate on table, soldering iron were checked.
- d. The well-grounded wristband was worn to remove static charges from our body.

- e. SuperSafe flux was used for even spreading. Care was taken not to put any extra solder/flux for soldering any of the component.
- f. When the solder melted, transistor was placed on the PCB using grounded tweezers.

8. Connector soldering:

Two radial connectors with 3mm long Teflon for both input and output were connected. M 2.5 screws were used to fix them. The center pins were soldered onto input and output 50Ω lines with minimum solder and flux. Extra flux was cleaned using IPA, Cotton and toothpick.

9. Coupling capacitor soldering:

- a. The coupling capacitors were placed exactly in the specified position.
- b. Both sides were soldered with minimum solder and flux.
- c. Extra flux was cleaned using IPA, Cotton and toothpick.

10. Bias wire and transistor lead soldering:

- a. Solder one end of the Gauge 30 Gold plated Copper wire on top of the 1.1pf bypass capacitor.
- b. The transistor holder was tightened with nut and washer at the bottom of the chassis using right spanner.
- c. The other end of the bias wire near the gate/drain leads were soldered using solder and flux at the low impedance portion of the input matching section.
- d. Extra flux was cleaned using IPA, Cotton and toothpick.

11. Cleaning:

- a. It was cleaned with alcohol.
- b. It was allowed to dry and checked for performance.

6.2 Experimental setup for the measurement of Gain And Return Loss of the amplifier

Experimental setup for the measurement of Gain and Return loss of the LNA is as shown in figure 6.3. It consists of a scalar network analyzer (HP 8757D), a synthesized sweeper (HP 83752A), directional bridge and a detector.

Initially the setup was made without connecting the LNA. The frequency range is set between 0.5GHz to 1.5 GHz

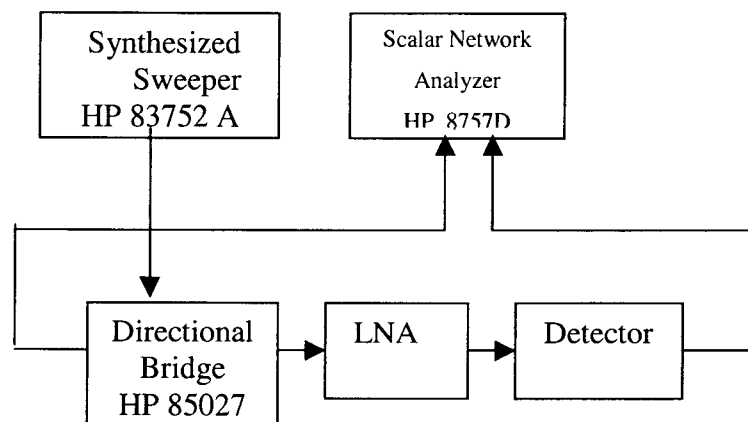
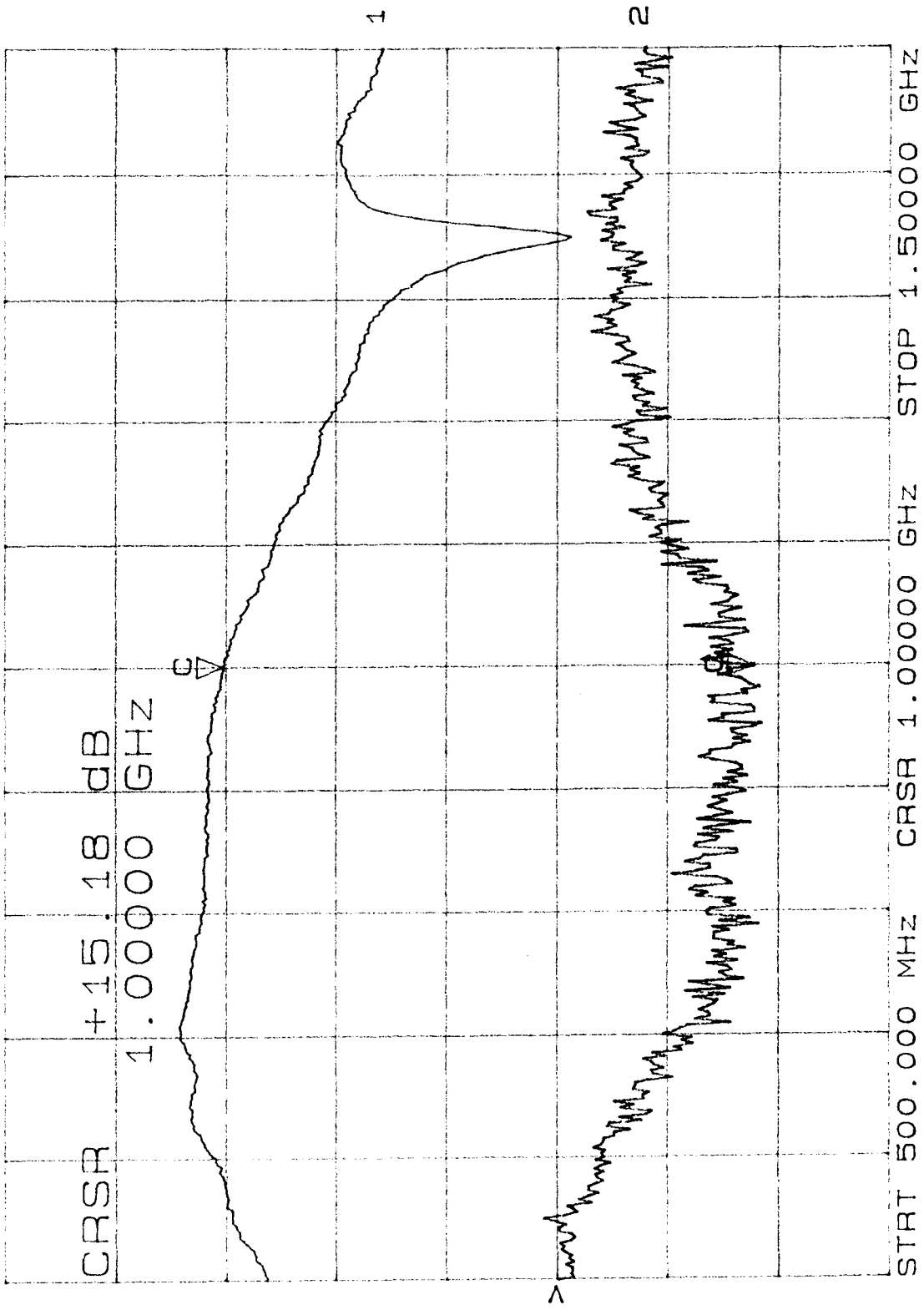


Fig 6.3 Experimental setup for Gain and Return loss

The power level was set to -35dBm. The system was calibrated to remove the instrumental effects. Then the LNA is connected in between the detector and the auto tester in the setup. Gain and return loss of the amplifier are measured and the plots obtained are shown in Fig 6.4

CH1: A --M A +15.18 dB
5.0 dB/ REF 0.00 dB

CH2: B --M A -8.87 dB
5.0 dB/ REF .00 dB



12 >

27 May 04 11: 55: 39

6.3 Experimental setup for the measurement of Noise figure of the amplifier

Experimental setup for the measurement of Noise Figure of the LNA is as given in figure 6.6. It consists of a Noise Figure Meter (HP 8970B) a Synthesized Sweeper.

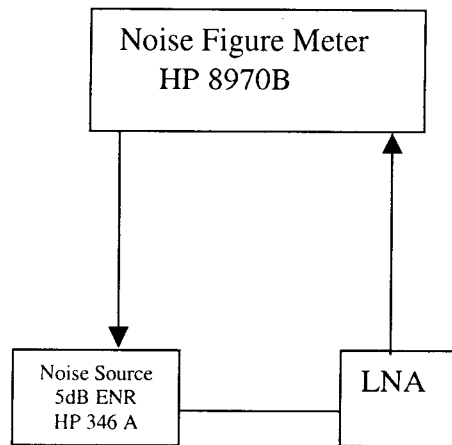
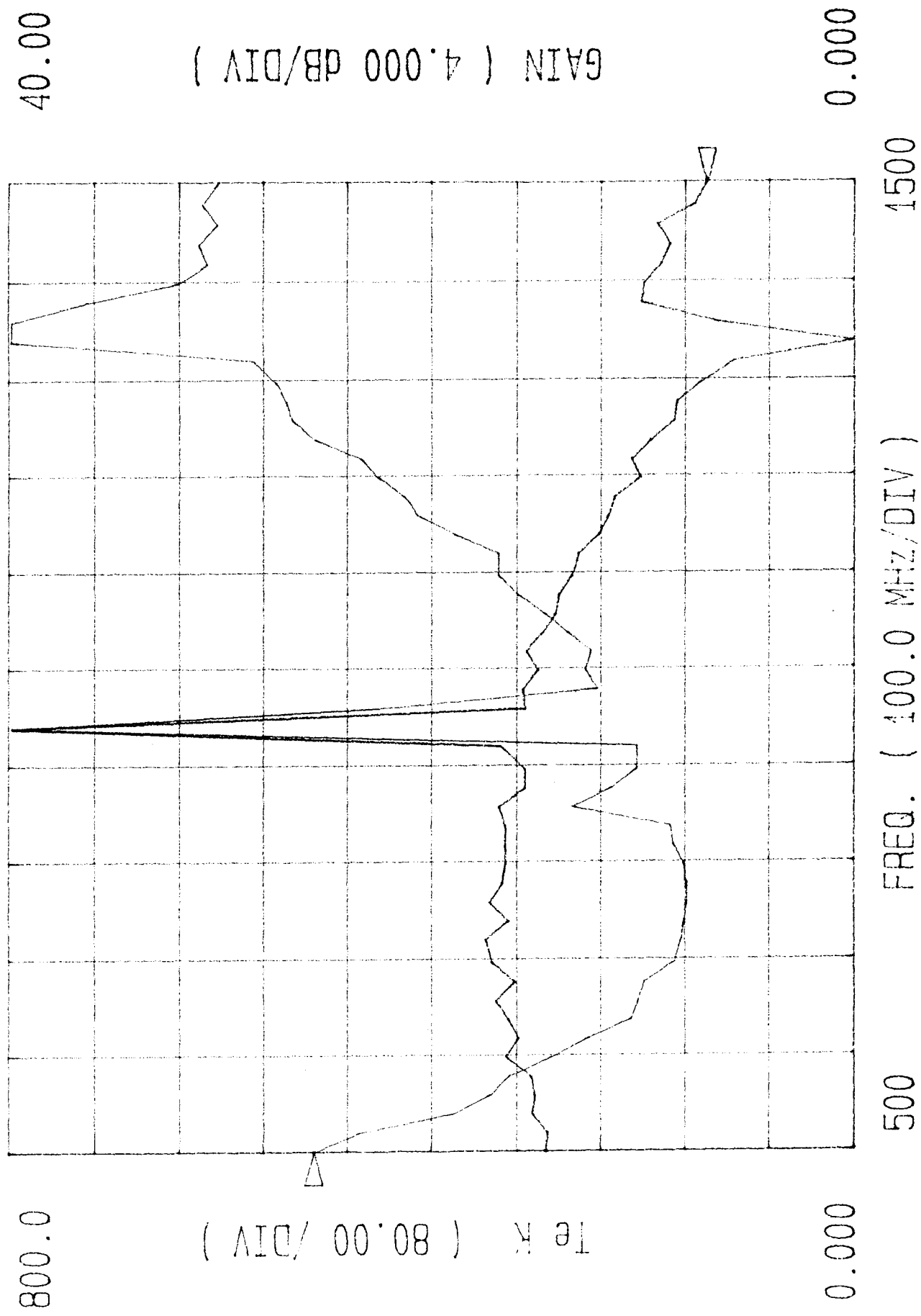


Fig 6.6 Experimental setup for Noise Figure

HP8970B Noise Figure Meter



CONCLUSION

We have developed successfully a multioctave bandwidth amplifier to operate in the frequency range of 0.5 to 1.5 GHz .We were able to get expected gain and the return loss over 0.5 to 1.3 GHz.

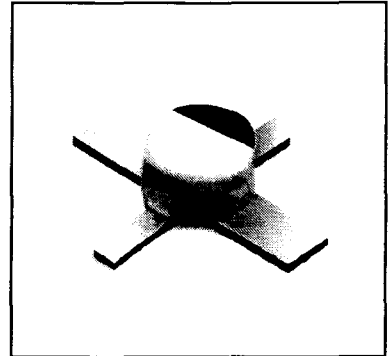
But the noise performance of the amplifier had deteriorated to a larger extent. Even though we had aimed at cooling the amplifier to the cryogenic temperature, due to some technical problems we were not able to cool .If the amplifier is designed carefully and cooled to low temperature, it can be used to cover a wide range of frequencies in the radio telescope.

FHX35X/002 FHX35LG/002

Low Noise HEMT

DESCRIPTION

The FHX35X/002 Chip and FHX35LG/002 packaged devices are HEMT (High Electron Mobility Transistor) ones suitable for use as the front end of an optical receiver in high speed lightwave communication systems. This HEMT combines high transconductance, low gate capacitance and low leakage current; all important factors in achieving low noise preamplification. Fujitsu's stringent Quality Assurance criteria and detailed Test Procedures assure Highest Reliability Performance.



LG PACKAGE

FEATURES

- High Transconductance
- Low Leakage Current
- Low Gate Capacitance
- Gold Bonding System
- Proven Reliability

ABSOLUTE MAXIMUM RATINGS (Ambient Temperature $T_a=25^\circ\text{C}$)

Item	Symbol	Conditions	Ratings	Unit
Drain-Source Voltage	V_{DS}		6	V
Gate-Source Voltage	V_{GS}		-5	V
Total Power Dissipation	P_T		290	mW
Storage Temperature	T_{stg}		-65 to 175	$^\circ\text{C}$
Channel Temperature	T_{ch}		+175	$^\circ\text{C}$
Thermal Resistance	R_{th}	Channel to Case	150	$^\circ\text{C/W}$

ELECTRICAL CHARACTERISTICS (Ambient Temperature $T_a=25^\circ\text{C}$)

Item	Symbol	Conditions	Limits			Unit	
			Min.	Min.	Max.		
Drain Current	I_{DSS}	$V_{DS}=2\text{V}, V_{GS}=0\text{V}$	15	40	85	mA	
Transconductance	g_m	$V_{DS}=2\text{V}, I_{DS}=10\text{mA}$	45	60	-	mS	
Pinch-off Voltage	V_p	$V_{DS}=2\text{V}, I_{DS}=1\text{mA}$	-0.2	-1.0	-2.0	V	
Gate-Source Leakage Current	I_{GSO}	$V_{GS}=-2\text{V}$	-	10	20	nA	
Gate-Source Capacitance	C_{GS}	$V_{DS}=3\text{V}$ $I_{DS}=10\text{mA}$	FHX35X/002	-	0.27	-	pF
			FHX35LG/002	-	0.47	-	
Gate-Drain Capacitance	C_{GD}	$V_{DS}=3\text{V}, I_{DS}=10\text{mA}$	-	0.035	-	pF	

FHX35X/002 FHX35LG/002

Low Noise HEMT

Fig. 1 Drain Current vs. Drain-Source Voltage

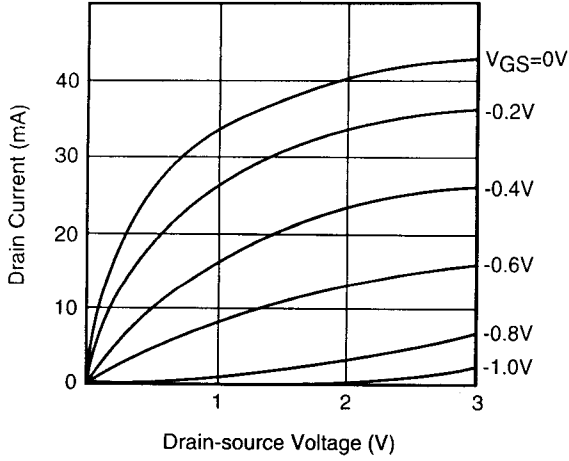


Fig. 2 Gate-Source Capacitance vs. Drain-Source Current

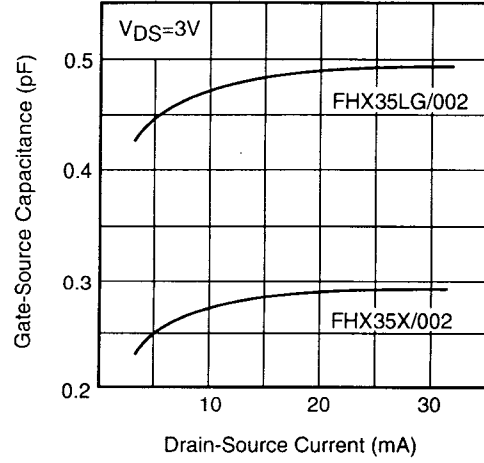


Fig. 3 Transconductance vs. Gate-Source Voltage

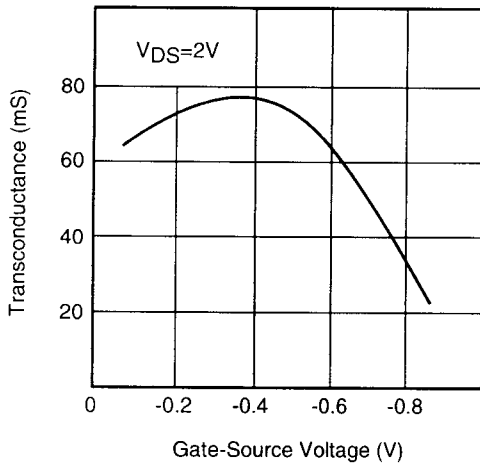
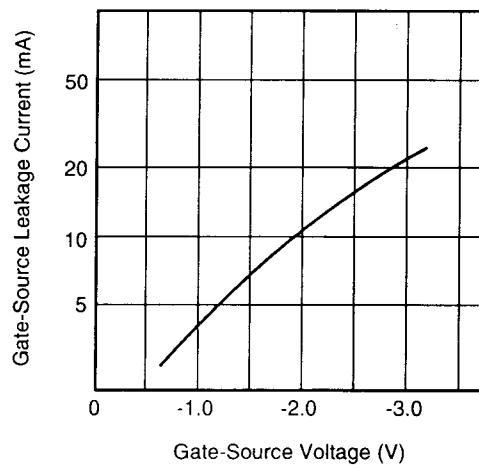


Fig. 4 Gate-Source Leakage Current vs. Gate-Source Voltage



8. Bibliography

1. Low noise microwave transistors and amplifiers
Edited by
Hatsuaki Fukui
A vol in IEEE press
2. Microwave Transistor Amplifiers,
Guillermo Gonzalez,
Prentice-Hall, Inc., Eaglewood Cliffs, N.J.,
1984.
3. Radio Astronomy,
John D Krause
Mc Graw-Hill Book Company,
1966
4. Microwave Devices and Circuits,
Samuel.Y.Liao,
Prentice-Hall, Inc., Eaglewood Cliffs, N.J.,
1980.
5. Principles of microwave measurements
GH Bryant
IEE Electrical Measurements series 5
6. Ultra low noise 1.2-1.7 GHz cooled GaAs FET amplifiers,
IEEE Transactions Microwave Theory And Techniques,
VOL MT1-30, NO-6, June 1982
7. The RF and Microwave Circuit Design cookbook
Stephen A Maas

8. Marian W. Pospie Zalski (senior member),
IEEE, Sander Weinreb, Fellow, IEEE, Roger D. Norrod,
IEEE member and Ronal Harris,
FET's and HEMT's at cryogenic temperatures- Their properties and use in Low
Noise amplifier, VOL-36, NO-3, March 1988.

9. S parameter design
Hewlett Packard application note 154
1972

10. Fujitsu Microwave Semiconductor Databook
1997

11. Marian W. Pospie Zalski (senior member), IEEE, Modeling of noise parameters of
MESFET's and MODFET's and their frequency and temperature dependence, Vol-
37, NO-9, September 1989.

12. Microwave Engineering,
David M Pozar

13. Raul Pettai, Noise in receiver systems

14. Sadik P.B, Cochin university of science,
Low Noise HEMT amplifier for Radio astronomy (Thesis).

9. Appendix

DC BIAS REGULATOR CIRCUIT OPERATION

The heart of the servo system lies in the ramp generator op amp 04(Quad TL084). Let us assume P2 is a 10K (wire wound) potentiometer. With the pot set at maximum value (with the dial at 30). Let us say that 30mA should be drawn by the FET (even though the FET will not be operated at this current, it induces that the current can be said set with the dial on the pot). Therefore -15V will be set on the inverting terminal of 04 and it ramps positively. This increases the gate voltage and the FET begins to draw more current through the transistor T1 and this current drops a voltage across the 200Ω resistor at its path. (The drain voltage is set by 02, but most of the current is taken from T1). The drop across the 200Ω is applied to the difference amplifier 03 and it produces a positive voltage at its output, proportional to the current through the GaAs FET. When this voltage reaches a value, it makes the ramp generator 04 to ramp in the opposite sense. Finally at steady state, the current charging the capacitor across 04 should be zero. This is possible only when

$$\frac{\text{Output of 03}}{100\text{K}} = \frac{\text{Setting of pot P2}}{500\text{K}}$$

$$\text{Output of 03} = \frac{15 \times 100}{500} = 3\text{V}$$

which is equal to the drop across the 200Ω showing that 30mA is flowing through the 200Ω and hence through the GaAs FET.

